MICROMECHANICAL EVALUATION OF INTERFACIAL SHEAR STRENGTH OF CARBON/EPOXY COMPOSITES USING THE MICROBOND METHOD

by

BETHANY WILLARD

B.S., Kansas State University, 2011

A THESIS

submitted in partial fulfillment of the requirements for the degree

MASTER OF SCIENCE

Department of Mechanical and Nuclear Engineering
College of Engineering

KANSAS STATE UNIVERSITY
Manhattan, Kansas

2013

Approved by:

Major Professor
Kevin Lease

Copyright

Abstract

Carbon fiber reinforced composites (CFRP's) are a mainstay in many industries, including the aerospace industry. When composite components are damaged on an aircraft, they are typically repaired with a composite patch that is placed over the damaged material and cured into the existing composite material. This curing process involves knowledge of the curing time necessary to sufficiently cure the patch. The inexact nature of curing composites on aircraft causes a significant waste of time and material when patches are unnecessarily redone. Knowing how differences in cure cycle affect the strength of the final material could reduce this waste. That is the focus of this research.

In this research, the interfacial shear strength (IFSS) of carbon fiber/epoxy composites was investigated to determine how changes in cure cycle affect the overall material strength. IFSS is a measure of the strength of the bond between the two materials. To measure this, the microbond method was used. In this method, a drop of epoxy is applied to a single carbon fiber. The specimen is cured and the droplet is sheared from the fiber. The force required to debond the droplet is recorded and the data is analyzed.

The IFSS of AS4/Epon828, T650/Epon828, and T650/Cycom 5320-1 composites were evaluated. For the former two material systems, a cure cycle with two steps was chosen based on research from others and then was systematically varied. The final cure time was changed to determine how that parameter affected the IFSS. It was found that as the final cure time increased, so did the IFSS and level of cure achieved by the composite to a point. Once the composite reached its fully cured state, increasing the final cure time did not noticeably increase the IFSS.

For the latter material system (T650/Cycom 5320-1), the two cure cycles recommended by the manufacturer were tested. These had different initial cure steps and identical final cure steps. Although both cure cycles caused high IFSS, the cycle with the higher initial temperature, but shorter initial cure time achieved a higher level of cure than that with a longer time, but shorter temperature.

Table of Contents

List of Figures

List of Tables

Acknowledgements

First, I would like to thank Dr. Kevin Lease for providing the opportunity to do this research. As my Major Professor, Dr. Lease provided not only lab space, equipment and funding, but invaluable support, knowledge, guidance, and patience throughout my research as well. A portion of this work was funded by NASA EPSCoR Grant #NNX11AM08A supervised by Wichita State University.

Thank you to Dr. Amy Betz, and Dr. Gurpreet Singh for serving on my committee and for the support and use of lab time and equipment. Thank you to Lamuel for helping obtain photos with the SEM. Your time and expertise was greatly appreciated. Also, thanks to Liz and Nassim, my lab mates, for your advice, assistance, and answers to questions along the way.

Last, but not least, thanks to my husband and family for your constant support and encouragement. You are a great support system and I am truly grateful for you!

Chapter 1 - Introduction

Background and Motivation

Composite materials have gained popularity in many applications over the past few decades. The aerospace, medical, construction, and plastics industries are just a few examples of the growing number of applications for which composites are being used. Composites are materials made of two or more different materials, and have properties distinctly different from the constituent materials. Carbon fiber reinforced polymers (CFRP's) are a category of composites made of carbon fibers and a polymer matrix material, usually an epoxy. These composites are typically stronger and more durable, yet lighter in weight than the materials they are used in place of. Another advantage is that the mechanical properties of composites can typically be customized for the specific application they will be used for. By changing the fiber or the matrix, the properties of the final composite can be significantly altered.

One application of CFRP's in the aircraft industry is using composite patches to repair damaged composite aircraft panel structures. Although the use of CFRP patches is quite common, the patching process itself makes it difficult to know the exact cure cycle the patch actually sees. In most patch techniques, the patch needs to be cured under vacuum at a specific temperature. This requires a type of vacuum bag and heat blanket system with thermocouples to assess the temperature of the patch during cure. With the less-than-ideal cure system, it is difficult to follow a strict cure cycle and then be sure that the entire patch cures evenly. Therefore, if any patch or part of a patch sees a cure time or temperature outside a narrow specified range, it is either rejected, or reworked at the very least [1]. This can waste a large amount of time and materials since many of these patches are still probably safe to use. If there was a better understanding of how variations in cure cycle affect the strength of the composite patch, many of these patches could likely be used instead of being wasted.

Goals and Strategy

Based on the discussion above, the overall goal of this thesis was to determine how cure cycle affects the strength of composite materials. Although this could be carried out using ASTM standard test specimens, this approach requires a large amount of materials. Evaluating these large macroscopic specimens does not give a small-scale view of how the cure cycle

affects the strength at the fiber/matrix level. Interfacial shear strength (IFSS) is a measure of the strength of the bond between the fiber and matrix in a composite material. Since the properties of the composite as a whole depend largely on the interface between the materials [2], testing the materials at the micromechanical level and finding the IFSS is a good indicator of how the overall composite material will behave. Based on this, the specific goal of this research was to use the microbond test to evaluate how the cure cycle affects the IFSS for a variety of CFRP material systems.

This research was carried out using three material systems: AS4/Epon828, T650/Epon828, and T650/Cycom 5320-1. For all material systems, the cure cycle consisted of an initial cure (time, temperature) and a final cure (time, temperature). For the AS4/Epon828 and T650/Epon828 material systems, the cure cycles were changed systematically by modifying the final cure time. For the T650/Cycom5320-1 material system, two cure cycles were used, both recommended by the manufacturer.

This thesis is organized into six chapters, including this introduction. The remaining five chapters are introduced here:

Chapter 2 includes an overview of testing techniques used to evaluate IFSS as well as a literature review of work others have done with CFRP's and the microbond method.

Chapter 3 describes the materials used and how the test specimens were prepared for each material system.

Chapter 4 describes the microbond test set-up and procedure in detail, and tells how it was applied to the specimens in this research.

Chapter 5 shows results from the microbond tests performed and discusses how the results compare to both others in this research and those obtained by other researchers.

Chapter 6 includes conclusions drawn from the current research as well as recommendations for further research in this field.

Chapter 2 - Literature Review

This chapter summarizes several of the most common testing techniques used for experimentally characterizing the interfacial shear strength in polymer-based fiber reinforced composite materials. It also discusses the work of several other researchers who used the microbond test to analyze carbon/epoxy material systems and/or the effect of cure cycle on the interfacial shear strength of polymer-based composites.

Techniques

Interfacial shear strength for fiber reinforced composite materials is typically determined experimentally using one of four main methods. They are single-fiber fragmentation, fiber push-out, fiber pull-out, and microbond tests. All four methods are discussed here briefly, while the microbond test (used in this project) is discussed in more detail in Chapter 4.

Single-Fiber Fragmentation Test

Kelly and Tyson [3] developed the single-fiber fragmentation (SFF) test (sometimes referred to as the single filament critical length method) in 1965 to look at the characteristics of copper specimens reinforced with either discontinuous or continuous tungsten or molybdenum wires [4]. This test uses a single fiber embedded in a dogbone-shaped matrix specimen, as shown in Figure 2.1a. After the specimen has been cured, a tensile test is run on it. For this tensile test, the force is applied to the shoulders of the specimen so that an external tensile force is not directly applied to the fiber. The tensile stress in the matrix is transferred to tensile stress in the fiber through shear stress at the fiber/matrix interface. As the tensile stress in the fiber increases and reaches the fiber ultimate strength, the fiber breaks into fragments. This fragmentation process continues until all fragments are too short to build up enough tensile stress to reach the ultimate tensile stress of the fiber. At this point, the specimen is said to have reached "saturation". The small segments are then measured, and the critical length is calculated from the average fiber fragmentation length [5]. The critical length of the fiber is the length at which applying more force to the specimen does not induce further fiber fragmentation. A saturated specimen is illustrated in Figure 2.1b.

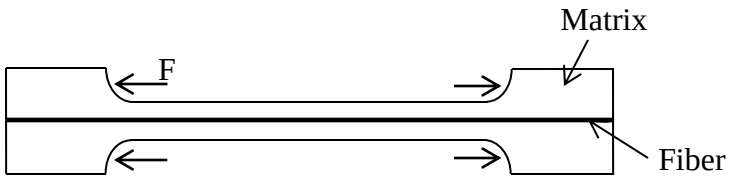

(a) Loading the SFF specimen

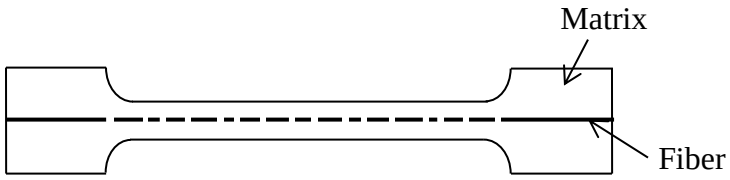

(b) Saturated SFF specimen

Figure 2.1 Schematic of the SFF specimen (a) before testing, and (b) after testing

The critical length is then used to calculate the interfacial shear strength using Eq. (1)

$$\tau = \frac{\sigma_f d}{2 l_c} \qquad (1)$$

where σ_f is the ultimate strength of the fiber, d is the diameter of the fiber, and l_c is the critical fiber length [6]. While this test is favorable in the fact that it can provide a relatively quick qualitative comparison between specimens and it mimics closely the actual loading a fiber would experience in a composite specimen, it also has some drawbacks. A few disadvantages that Bradford [5] discussed were that the calculation of the IFSS may be oversimplified, the matrix needs to have a significantly higher strain limit than the fiber, and the strength of the fiber at the critical length needs to be known.

Fiber Push-Out Test

The fiber push-out technique (sometimes referred to as the microdebonding test [4] or the microcompression test [5]) was developed by Grande [7] in 1980. He developed this in order to have a test method that could qualitatively measure the strength of the fiber/matrix interface. Grande used S-Glass/Epoxy and Graphite/Epoxy material systems in his work. The fiber push-out technique uses a fiber embedded in a block of matrix. The specimen is prepared and then cured. For the test, a very small, sharp object (usually diamond-tipped) is brought into contact with the fiber and applies a downward force until the fiber debonds and moves through the matrix. A schematic of the test is shown in Figure 2.2.

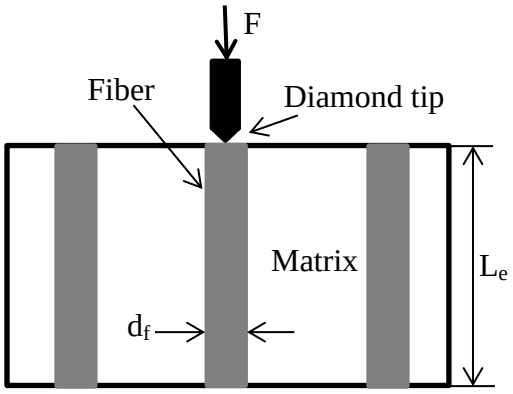

Figure 2.2 Fiber push-out test set-up

After the test is run, the interfacial shear strength can be found by using Eq. (2) [2]

$$\tau_{IFSS} = \frac{F_{max}}{\pi d_f L_e} \qquad (2)$$

Where F_{max} is the force it takes to debond the fiber from the matrix, d_f, is the fiber diameter, and L_e is the embedded length. Like the SFF test, the fiber push-out test also allows testing of the fiber/matrix interface in a real composite environment [5]. Some disadvantages for this method are the test set-up and procedure, difficulty in measuring the fiber diameter [4], inability to see the failure mode [5], and making sure the fiber type used is hard enough not to split under the diamond tip [2].

Fiber Pull-Out Test

The fiber pull-out technique is similar to the fiber push-out technique, except, as the name suggests, the fiber is pulled out of the matrix instead of pushed through. This test was developed in 1969 by Broutman to study boron filaments [8]. For this method, the end of the fiber is embedded in a block of matrix, as shown in Figure 2.3. The matrix block is then secured to a testing device, and a force pulls on the fiber until debonding occurs and the fiber pulls out of the matrix block. The debonding force is then used in Eq. (2) to calculate interfacial shear strength [2].

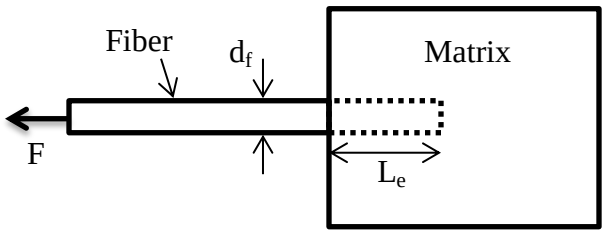

Figure 2.3 Fiber pull-out test set-up

One major disadvantage to the fiber pull-out test is that it cannot easily be used with very small fibers (such as carbon fibers). If the embedded length is too large, the interfacial shear strength will be greater than the tensile strength of the fiber, and the fiber will break before debonding occurs [9]. This can be solved by using a smaller block of matrix, but when the block is small enough to use with the smaller fibers (carbon or glass, for example), the thin meniscus formed becomes a significant percentage of the embedded length and can break during testing prior to debonding. Also, aligning the fiber properly in the matrix can be difficult, and that alignment has a large impact on the test results.

Microbond Technique

The microbond test is a variation of the fiber pull-out test, and is sometimes referred to as the microdroplet test. Miller et al. [9] developed the microbond test in 1987 as a better alternative to the fiber pull-out test. They proposed that the microbond test could be used with smaller fibers (ex. carbon, glass, Aramid) and would solve the problem of a large meniscus forming on the fiber in preparing specimens for the pull-out test. Most of their work was performed on E-glass/Epon828 specimens, but they also ran tests using Kevlar49/Epon828 and Celion3000/Epon828 material systems. In this method, a single droplet of matrix is deposited on a single fiber, and the specimen is cured. One end of the fiber is then secured to the testing device, and knife edges pull on the droplet until it debonds from the fiber. The force it takes to debond the droplet is recorded and used in Eq. (2) to calculate the interfacial shear strength. The test set-up is shown in Figure 2.4. It should be noted that Eq. (2) was developed using a shear lag model, which assumes the IFSS is uniform across the fiber/matrix interface. The actual IFSS is likely not uniform, however, and is discussed further in the summary of the paper by Kang et al. [10] in the next section of this chapter.

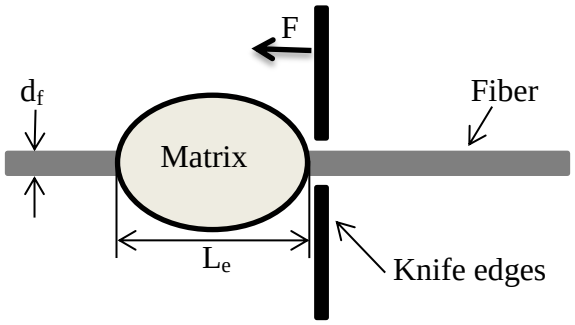

Figure 2.4 Microbond test set-up

The microbond technique was chosen for this research since it is a relatively quick and simple method to find interfacial shear strength [11]. Also, the test can be used for most fiber/matrix systems [5], and the equipment was available in the lab as another student in the research group had already developed the testing device [2]. One disadvantage is that the failure mode of the specimen is difficult to see based on the small size of the specimens [5]. Although relatively inconvenient, this problem can be solved by looking at the specimens with an SEM microscope after testing. The microbond method used is discussed in further detail in Chapter 4.

The next section presents research performed by others using the microbond method to study similar material systems and/or how cure cycle affects the interfacial shear strength of polymer composites. Since the next section includes a brief literature review of the microbond test, it is of interest here to introduce typical results and graphs reported from the tests. First, Force vs. Time or Force vs. Displacement graphs made from the raw data show what happened during the test. A typical Force vs. Displacement graph is shown in Figure 2.5 [10]. The initial portion of the graph where the slope is steep is where the knife edges were in contact with the droplet. The point at which the load instantly drops (F_d) on this graph is where the droplet debonded from the fiber. The portion after that where the load increases again to a constant, low level is the frictional force that occurred when the droplet slid along the fiber after debonding. This debonding force is used to plot the Force vs. Embedded Length and Force vs. Embedded Area graphs discussed next.

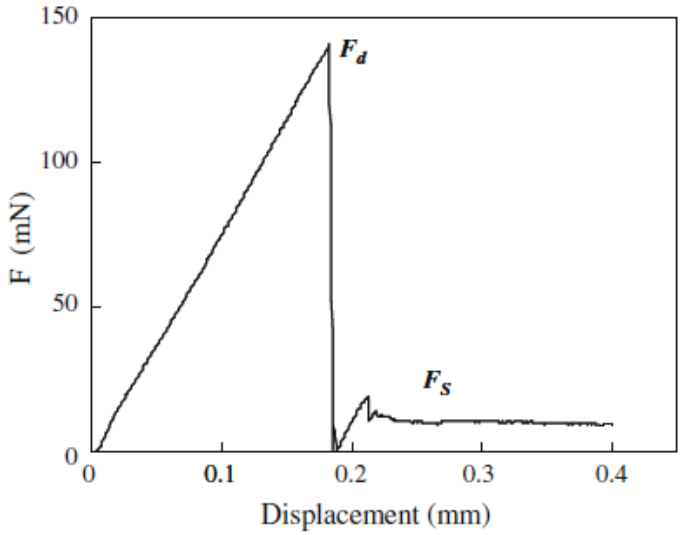

Figure 2.5 Typical Force vs. Displacement graph made from raw test data (graph taken from [10]).

The two graphs used to then analyze the data are Force vs. Embedded Length and Force vs. Embedded Area. Each point on these graphs is plotted using the debonding force (F_d shown in Figure 2.5) from a specimen against either the embedded length or area for that specimen. Typical examples of these graphs are shown in Figure 2.6 and Figure 2.7. (Although fiber breaks often occur at large embedded lengths, they are typically not shown on the graphs as seen in Figure 2.6.) Both types of graphs can be used to find the IFSS of the system. The methods to obtain the IFSS using the graphs are described in more detail in the next section.

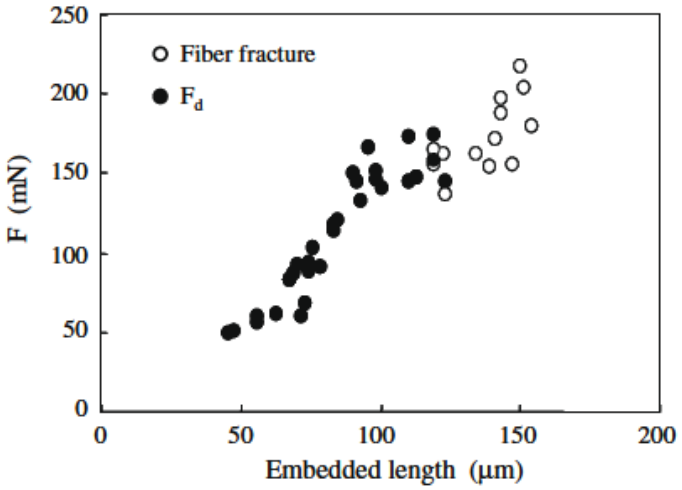

Figure 2.6 Typical Force vs. Embedded Length graph (taken from [10]).

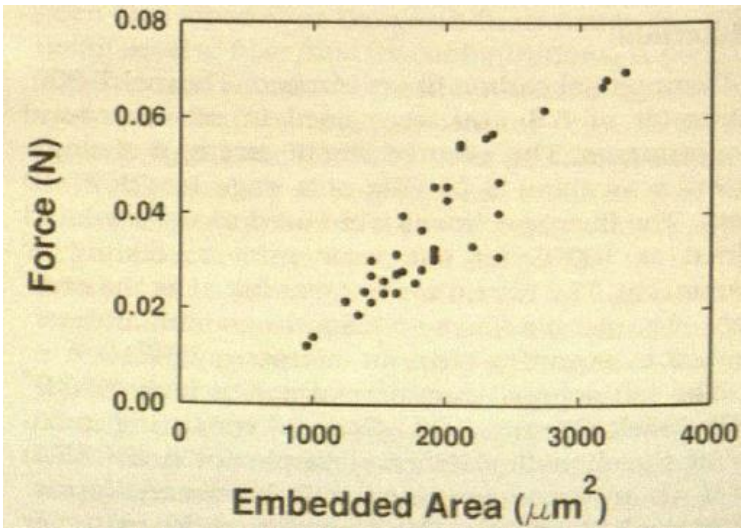

Figure 2.7 Typical Force vs. Embedded Area graph (taken from [11]).

Selected Results from Others

The microbond technique has been used extensively by others to study the strength of the bond between the fiber and matrix. This section provides examples of specific cases where researchers used the technique to study systems similar to those used in this research and/or look at the effects of different cure cycles on the composite.

Kang et al. [10] used an AS4/Epon828 material system and the microbond technique to compare experimental microbond results with those from a finite element analysis study. AS4 is a common aerospace grade, high strength, standard modulus carbon fiber, and Epon828 is a commonly used thermoset resin. These two materials are discussed in more detail in Chapter 3. First, they looked at two different methods of calculating IFSS from the experimental microbond data. The first, and most widely used method [12], was using the average of the values they calculated from their data set using Eq. (2). The second method was to use regression analysis to find the slope of the line of their Force vs. Embedded Length graphs, as seen in Figure 2.8 [10]. The slope of the line (F_{max}/L_e) was then divided by $\pi * d_f$ to obtain the IFSS value. (The same result could also be found using a regression line through data in a Force vs. Embedded Area graph and would require no further calculation.) In Figure 2.8a, the regression line was applied to the entire data set and forced through zero. This was done to agree with the equation and physical sense. If there is zero embedded length, the debonding force, and therefore the IFSS,

would also be zero. In Figure 2.8b, they made several regression lines based on trends they saw in the data (without forcing them through zero), but the most useful is regression line 2. It is based on the total data similar to regression line 1, but not forced through zero. This represents a true average of the data points themselves without taking into account what should be happening based on the equation.

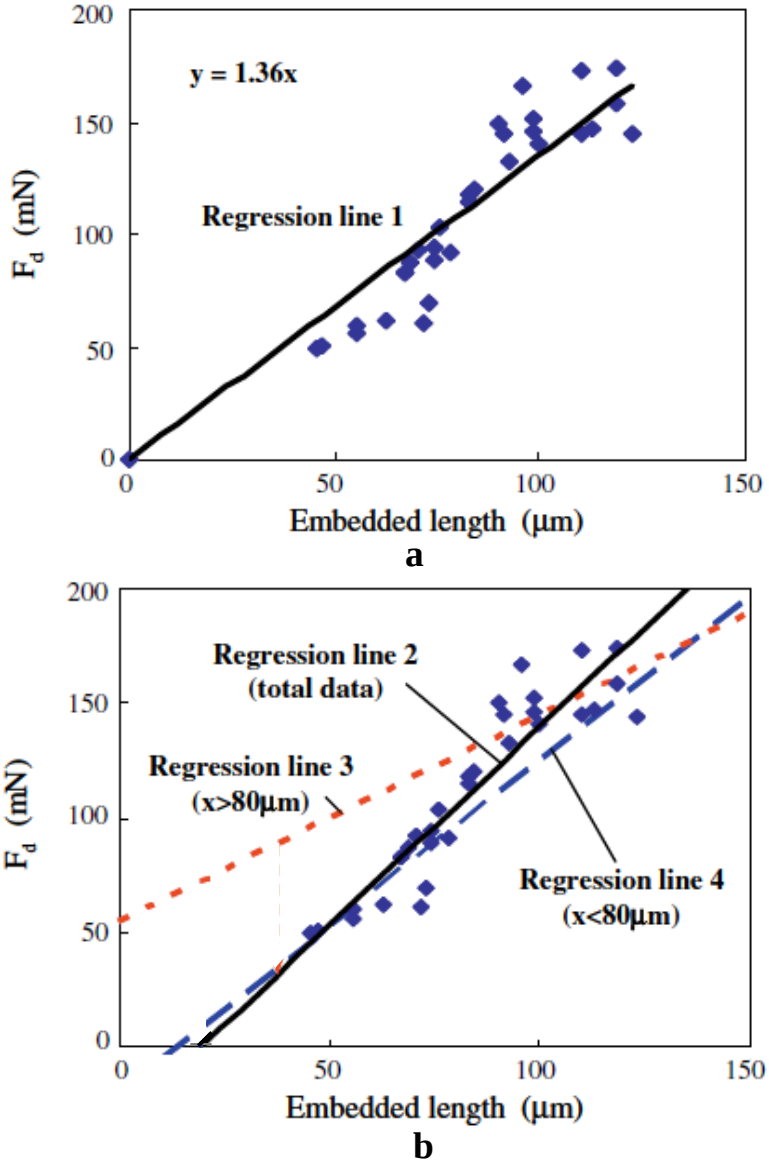

Figure 2.8 Regression analysis for AS4/Epon828 system reported by Kang et al. (a) Regression line forced through zero. (b) Regression lines based on data trends and total data not forced through zero. (Adapted from [10])

They saw that the IFSS found from the average of the numerical values in the first method and that found from Figure 2.8a were very similar, but the strength from regression line 2 was significantly higher, as shown in Table 2.1 (adapted from [10]). They hypothesized that the higher slope from regression line 2 (Figure 2.8b) was most likely due to the behavior of the stress concentration in the smaller droplets. The meniscus of a smaller droplet makes up a larger percentage of its overall embedded length, and therefore the smaller droplets are usually more oblong than the larger, more spherical droplets. If the width of the knife edges is relatively constant for all droplets, smaller droplets would have less area in contact with the knife edges, and would therefore have a higher shear stress concentration, causing them to potentially fail at lower loads than expected.

Table 2.1 Interfacial shear strengths for various methods discussed: A) average using Eq. (2), B) regression line through origin (#1 in Figure 2.8a), and C) regression line not through origin (#2 in Figure 2.8b). (Table adapted from [10]).

τ_d	A	B	C
MPa	55.3	57.6	73.3

Kang et al. [10] also used finite element analysis to investigate whether the shape of the droplet had an effect on the IFSS. They used three droplet shapes: perfect sphere, typical droplet (mostly spherical, but with a meniscus), and perfect cylinder. In their basic analysis of IFSS, they found that the typical droplet shape had the highest average strength at 66.6 MPa, the spherical model was a close second at 66.1 MPa, and the cylindrical model had the lowest average IFSS with 59.6 MPa. This shows that droplet shape has some effect on the IFSS values and may account for some scatter in the data, but all still give a fairly accurate representation of the IFSS.

They took their FEA analysis one step further to look at the validity of the shear lag model for Eq. (2). They did this by evaluating the octahedral shear stress and the distortion energy at and near the fiber/matrix interface. Figure 2.9 shows the IFSS distribution along the fiber/matrix interface of a droplet compared to the shear lag model used by Eq. (2) with the same embedded length and debonding force.

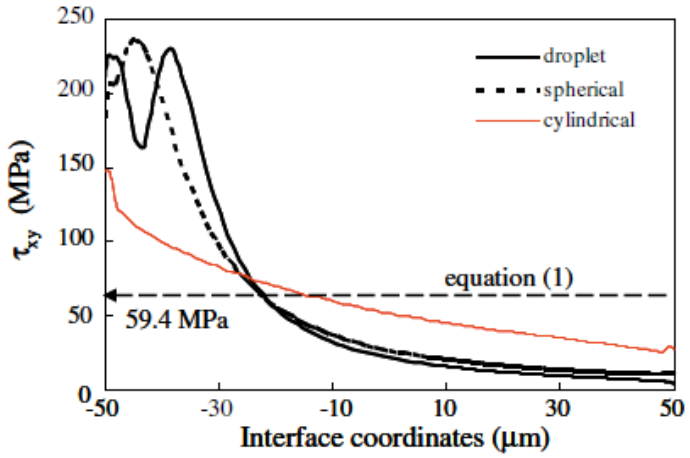

Figure 2.9 Distribution of shear stresses along the fiber-matrix interface [10].

This figure shows that the distribution of the shear stress along the fiber-matrix interface is not at all constant as is assumed by the shear lag model and Eq. (2), but the averages from the models (66.6 MPa, 66.1 MPa, and 59.6 MPa) are still very close to the IFSS of 59.4 MPa found using the equation. This result helps to validate using the shear lag model to develop the equation used most often to calculate IFSS. However, it is obvious that Eq. (2) does not take into account the high stress concentration shown at the knife edges.

Although they showed that the shear lag model provides a good approximation of the IFSS, Kang et al. [10] proposed that perhaps a better IFSS value (that attempts to take into account the stress concentration) could be obtained by calculating the average octahedral shear stress from the distortional energy in the FEA elements at the interface. They studied their model and came up with compensation factors based on the shape of the meniscus. The more "real" value of IFSS could then be found by simply multiplying the IFSS found using Eq. (2) by the appropriate correction factor for each droplet. The compensation factors for the droplet, spherical, and cylindrical models were 1.25, 1.16, and 0.90, respectively [10]. Although this is an interesting study, the compensation factors were not used in the research presented in this paper.

Biro et al. (1991) [11] used the microbond method to study the effects of cure cycle and an added fortifier with a T300/Epon828 material system. T300 carbon fiber is another common aerospace grade high strength, standard modulus fiber. It is very similar to the AS4 fiber but has a slightly lower tensile strength than the AS4 [13,14]. The Epon828 was used in its unaltered

form for a portion of the experiments (host system), but they also experimented with adding different amounts of a chemical fortifier to the resin (systems A and B) in an effort to change the IFSS. They found that both changing the cure cycle (cure cycles used are shown in Table 2.2 [11]) and adding fortifier in the resin affected the IFSS.

Table 2.2 Cure cycles used by Biro et al. (1991) (reproduced from [11])

Cure Schedule	Conditions
B-Staged	24 h @ room temperature
Cure I	24 h @ 60°C
Cure II	2 h @ 60°C, 2 h @ 120°C
Cure III	2 h @ 60°C, 2 h @ 120°C, 2 h @ 165°C
Cure IV	2 h @ 60°C, 1 h @ 120°C, 5 h @ 180°C

Biro et al. (1991) [11] also calculated the interfacial shear strength using the two methods outlined by Kang et al, except they did not specify whether the line of best fit was forced through the origin or not. A Force vs. Embedded Area graph is shown in Figure 2.10. This graph shows some scatter in the data. The researchers noticed similar scatter in their data for each individual system/cure cycle, which they attributed to variations in the fibers over short distances. This data looks as if a line of best fit would come close to having a zero-intercept, but would be too steep and actually cross the x-axis around 100-200 μm. They explained this offset as a standard deviation of the intercept caused by the small variation of embedded lengths, however.

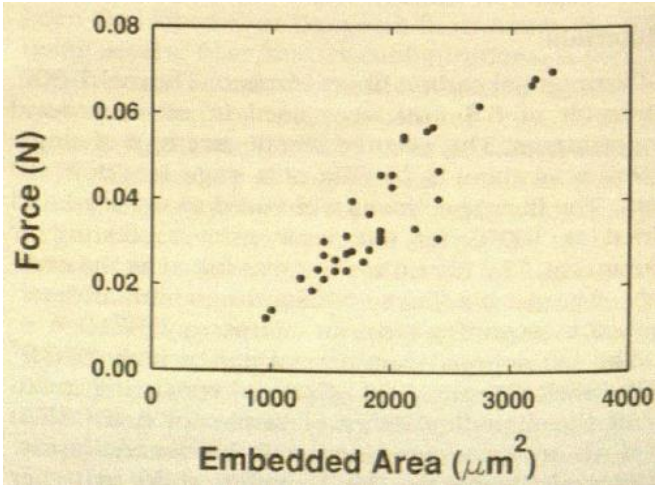

Figure 2.10 Force vs. Embedded Area graph of B-Stage, host system microbond test data collected by Biro et al. [11]

The IFSS value obtained by averaging the calculated strengths and that found from the regression analysis of the Force vs. Embedded Area graph were very close in all cases, differing by only 0.3-3.6 MPa. These values obtained from both the normal and fortified systems for all cure cycles are shown in Table 2.3.

Table 2.3 Interfacial shear strength values obtained by Biro et al. (1991) for both the regular (Host) and fortified (System A) material systems (reproduced from [11])

Formulation	Cure Schedule	τ_{avg} Average of Tests (MPa)	τ_{avg} From Slope of Regression (MPa)	N*
Host System	B-Stage	18.5 ± 3.7	19.5 ± 0.5	38
	Cure I	44.2 ± 11.8	43.3 ± 2.7	23
	Cure II	--	--	--
	Cure III	--	--	--
	Cure IV	50.2 ± 6.7	50.6 ± 1.2	33
System A	B-Stage	21.2 ± 4.5	20.7 ± 1.2	16
	Cure I	40.6 ± 7.8	43.3 ± 2.0	12
	Cure II	30.0 ± 9.0	26.4 ± 1.7	19
	Cure III	58.4 ± 12.8	61.4 ± 2.5	27
	Cure IV	66.6 ± 10.8	67.5 ± 1.3	53

Note: Variation is expressed as standard deviations

***Number of specimens.**

This data along with their discussion was slightly confusing. The researchers stated that for the host system, Cure I and II did not completely cure the epoxy, while Cure III and IV achieved a fully cured specimen. The level of cure achieved by the specimens for each cure cycle was determined using differential scanning calorimetry (DSC). Cure III and Cure IV had final temperatures which exceeded the glass transition temperature of the epoxy. The researchers noted that curing at a temperature above the glass transition temperature would likely "increase segmental chain motion of the cure network which may enhance the mechanical properties of the composite. [11]" Data, however, was only reported for B-Stage, Cure I, and Cure IV for this system. Although a little confusing, the results for both the host and fortified systems showed that the IFSS increased as the time and temperature of the final cure increased (see Table 2.2 and Table 2.3 [11]). The effect of cure cycle on the IFSS was significant, as the strength of the

specimens with the hottest and longest cure cycle (Cure IV) was two to three times that of the B-stage specimens within the same system.

Biro et al. (1991) [11] also briefly discussed what contributed to the IFSS and the types of bonds that occurred between the fiber and matrix at the interface. They state that there are three components to the adhesion between the two materials; mechanical, physical, and chemical. The chemical component could possibly consist of van der Waals forces, hydrogen bonds, or the stronger covalent bonds, but since the droplets tended to debond cleanly and not leave much, if any, resin behind, the weaker van der Waals forces are likely to be present rather than the covalent bonds. The mechanical interaction of simply having contact between the carbon surface and the cured epoxy also contributes to the overall IFSS.

Another point of discussion in this paper was about the role residual stresses played in the IFSS. They used the thermal expansion coefficient, Young's modulus, and Poisson's ratio of each of the materials along with the glass transition temperature and room temperature to find the residual stress in the specimen caused by cooling them down to room temperature. Although they were careful to cool the specimens slowly at a rate of <5°C/min, the residual stresses in Cure IV for each system accounted for approximately 20-30% of the IFSS of each system [11].

Biro et al. (1993) [12] did another study later using the microbond test to look at the effect that long term exposure to water had on the IFSS of AS4/Epon828 and T300/Epon828 composites. While the bulk of their paper was specific to the hygrothermal exposure and will not be discussed here, they did discuss some key points about the microbond test. These are summarized here. They again speculated that the complicated fiber/matrix interfacial interactions for AS4/Epon828 consisted of van der Waals forces, chemical bonding, and some mechanical interlocking between the resin and the fiber surface. They performed an X-ray photoelectron spectroscopy (XPS) study to obtain information about the "functional groups on the surface of carbon fibers [12]", and therefore have a better idea of the chemical bonding capabilities of the fibers. The XPS showed that the surface of the AS4 fibers contained a high amount of nitrogen as well as oxygen-containing species, which both contribute to reactions with epoxy. This fact, along with the visually smooth surface of the AS4 fiber, suggest that the van der Waals forces and chemical bonding likely contribute more to the IFSS than mechanical bonding between the materials. Another point of interest was that they also cited several sources for scatter in the data, including local variations in fiber surface, droplet shape, stress

concentration on the droplet, and the non-uniform stress distribution in the fiber/matrix interface [12].

In one of the first microbond tests performed, Miller et al. [9] used three different fiber/epoxy material systems each cured for 2 hours at 80°C, then 1 hour at 150°C. The first material system was an E-glass/Epon828 epoxy system. Once they saw the method gave comparable results to other IFSS test methods for similar systems, they then used Kevlar49 Aramid/Epon828 and Celion 3000 carbon/Epon828 specimens. E-glass is an inexpensive, high strength, high stiffness glass fiber commonly used in fiberglass and composites [15]. Kevlar is a high strength, high modulus fiber typically used in textiles, fiber optic cable, and marine and aerospace applications [16]. Celion 3000 carbon fibers are unsized high strength and high modulus fibers [17, 9]. For their tests, Miller et al. [9] placed two epoxy droplets per fiber. During testing, they brought the knife edges together until they barely touched the fiber, causing a small level of frictional force throughout the test. This allowed them to determine the failure mode (debonding, fiber break, or droplet slipping through knife edges) based on the Force vs. Displacement Graphs. The different traces for each failure mode are shown in Figure 2.11 [9].

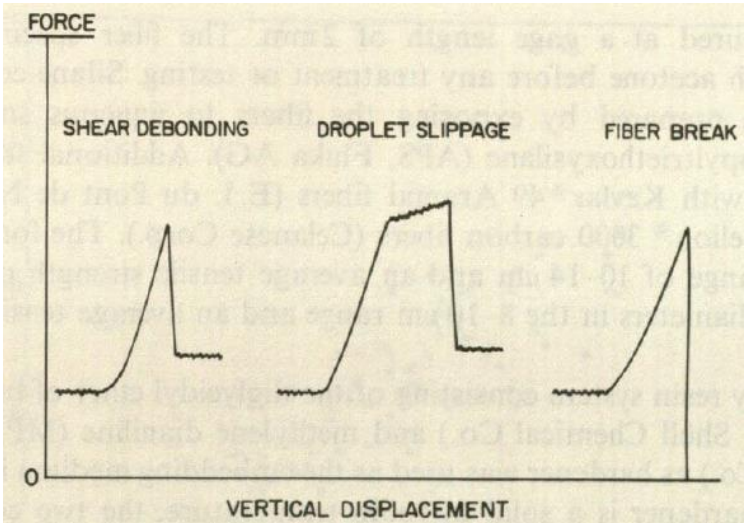

Figure 2.11 Force traces for the possible failure modes of a microbond test [9]

Although Miller et al. [9] cited these traces as a way to determine failure mode without having to look at each specimen under the microscope after testing, some later researchers have still done

post-measurement microscopy in order to determine the true embedded length if any matrix is left behind after the test [11,12].

Miller et al. [9] did two interesting studies with the E-glass/Epon828 specimens. First, they looked at the variation in IFSS values between droplets on the same fiber and compared it to the variation of the values for the whole test population for each set of resin. The results (shown in Table 2.4, reproduced from [9]) show that the variation in the values for droplet pairs was significantly lower than that from the population. Since droplets close together on the same fiber produced much closer IFSS values with each other than with droplets on other fibers, they concluded that a significant factor in the data scatter was due to variations in the surface characteristics of the fibers themselves. While they felt that the fiber surface was likely the greatest contributor to data scatter, the researchers acknowledged that variations in knife edge placement, droplet size measurements, and other such parameters could also cause some scatter in the data.

Table 2.4 Variations in Measured Bond Strengths (reproduced from [9])

Set	Average variation within pairs (%)	Coefficient of variation for total population (%)
I	8.2	22.5
II	8.9	16.8
III	10	15.2

The second item they investigated with the E-glass/Epon828 specimens was whether or not they could identify a trend for how IFSS changed with the amount of epoxy on the fiber. To do this, they graphed IFSS vs. Embedded Length, IFSS vs. Embedded Area, and IFSS vs. Droplet Volume and looked for trends in the data. They did not find any. They first thought they saw a trend that IFSS decreased with an increased amount of resin, but then decided that could be a misleading conclusion since the number of successful debonding tests diminished as the amount of resin increased as well. The values shown in Table 2.5 (reproduced from [9]) show how as the amount of resin (droplet size) increased, so did the number of fiber breaks during testing. This increase in fiber breaks as droplet size increased was also seen in the current research with carbon fiber/Epon828 specimens and will be briefly discussed in the Results and Discussion section.

Table 2.5 Incidence of Fiber Failure for Different Embedded Lengths (Glass Fibers) (reproduced from [9])

l (μm)	Fiber breaks/specimens
60-99	8/151
100-139	16/57
140-179	13/21

The Force vs. Embedded Area graph Miller et al. obtained for the Celion 3000/Epon828 system is shown in Figure 2.12 [9]. The average IFSS value for this system was about 57 MPa. While they acknowledged that the IFSS could be found by either averaging the values calculated using Eq. (2) or by a regression analysis on the Force vs. Embedded Area graph (the same methods used by Kang et al. [10] and Biro et al. [11]), they did not specify which method they used to obtain the average IFSS values they reported. The value of 57 MPa is comparable to those obtained by others using carbon/epoxy systems [10, 11, 12].

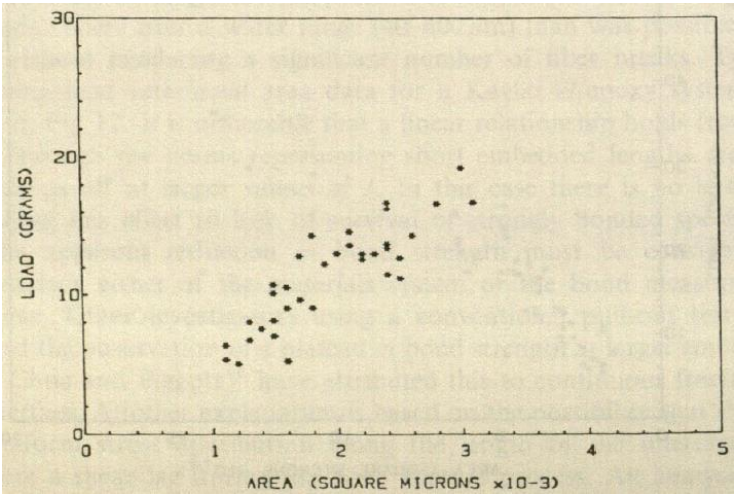

Figure 2.12 Debonding Load vs. Embedded Area: Celion 3000/Epon828 [9]

While not as drastic as the data from the E-glass specimens, the tapering of tested specimens as embedded area increased can be seen in the Celion 3000/Epon828 graph in Figure 2.12. Around 3000 μm^2, there are less data points than at areas smaller than that. This again is due to the IFSS approaching or exceeding the tensile strength of the fiber.

Miller later performed more microbond tests with Gaur to look further into the parameters of the tests. Gaur and Miller [18] used the same Kevlar 49/Epon828, E-Glass/Epon828, and Celion/Epon828 material systems as Miller et al. used in the paper discussed previously [9], but Gaur and Miller also added a Kevlar29/Epon828 material system. The cure cycle used for all specimens was 2 hours at 80°C followed by 2 hours at 150°C. This cure cycle is similar to that used by Miller et al., but includes one more hour at the higher temperature. Since three of the four material systems used by the two groups were the same, the results between the two papers should give some insight into how cure cycle affects the IFSS. In graphing IFSS vs. Embedded Area, the researchers saw a trend in data from both Kevlar material systems that they did not see in the E-glass or Celion system data. This trend showed that IFSS decreased as embedded area increased. From this data they concluded that the shear lag model is not a true representation of the force distribution during the test. Instead, as Kang et al. [10] also pointed out, the force is concentrated at the end of the droplet in contact with the knife edges and decreases as the distance from the knife edges increases. The trend was not seen in either the E-glass or the Celion material system data, however, so they concluded that embedded area has to increase significantly in order to see a downward IFSS trend (embedded area ranges: 1000-9000 μm^2 for Kevlar systems, 1500-4500 μm^2 for E-glass system, and 900-2700 μm^2 for Celion system) [18]. The latter two material systems had much narrower ranges of testable embedded areas due to the low tensile strength of the E-glass fibers and the high IFSS of the Celion/Epon828 system [18].

Gaur and Miller [18] used the same droplet/specimen set-up as Miller et al. [9]. They placed two droplets several millimeters apart on the same fiber. Miller et al. tested one droplet, retracted the knife edges, and then tested the second droplet. Gaur and Miller performed part of their tests that way, but some of their tests on the Kevlar49/Epon828 specimens were carried out with a "droplet shearing droplet" method, testing the first droplet, then letting the knife edges continue to move so the first droplet (now debonded) ran into the second droplet. The second droplet was then sheared by the force coming through the first droplet instead of from the knife edges themselves. They then compared the IFSS data from the first and second droplets to see if shearing the second droplet with the first instead of the knife blades affected the results. Their graph is shown in Figure 2.13 [18].

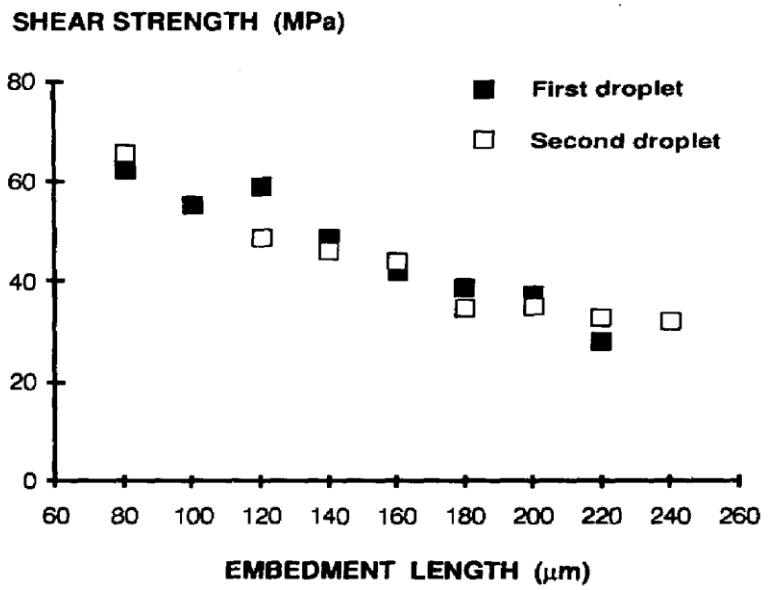

Figure 2.13 IFSS vs. Embedded Length graph comparing IFSS for first and second droplets in the "droplet shearing droplet" tests with the Kevlar 49/Epon828 material system (each point is an average of the data within a 20 μm range). [18]

From this graph, they concluded that there is no significant difference between the two data sets, so the shearing force from the knife blades or from a debonded droplet must be very similar. The researchers also felt these results validated the microbond method and the thought that the test measures a true shearing force between the materials since the geometry of the droplets in the "droplet shearing droplet" method should produce a predominantly shearing force [18].

Similar to Miller et al., Gaur and Miller [18] also looked at the differences of IFSS of droplets on the same fiber versus those on different fibers. They found the same results as the previous authors (droplets on the same fiber have IFSS closer to each other than to droplets on different fibers) and again concluded that differences in fiber surface play a significant role in data scatter.

Comparing the data from Miller et al. with that from Gaur and Miller, a brief conclusion can be drawn for how cure cycle affects IFSS. For the same Celion 3000/Epon828 material system, the first author obtained an IFSS of 57 MPa with a cure cycle of 2 hours at 80°C followed by 1 hour at 150°C [9], while Gaur and Miller found an IFSS of 65.3 MPa with a cure

cycle of 2 hours at 80°C followed by 2 hours at 150°C [18]. These numbers show that increasing the time of cure can increase the IFSS for a material system.

Ahmadi [2] also studied the effects of cure cycle on interfacial shear strength, but used a drawn glass fiber/PDMS system instead of a carbon/epoxy material system. Even though the material systems are different, data trends should still be similar. Ahmadi performed the microbond test on specimens cured with four different cure cycles and found IFSS increased as cure time and temperature increased, but plateaued at a certain point when the specimen became fully cured. This showed that increasing time and temperature increases the strength of the bond between the fiber and matrix, but once the matrix is fully cured, increasing these parameters no longer increases this strength.

Chapter 3 - Materials and Specimens

Fibers and Matrix Materials

Two types of commercially available high strength, standard modulus, PAN-based carbon fibers were used in this research. PAN-based fibers are made from a polyacrylonitrile (PAN) precursor that goes through a multi-step process. Many details in the fiber-making process are proprietary and specific to each company and fiber type, but the general process for making PAN-based carbon fibers is the same [19]. First, PAN is made by combining an acrylonitrile monomer with a catalyst. The PAN material then goes through a process called "spinning", where it is spun, extruded, stretched, and dried. This step forms the fibers into to correct size and shape. The fibers are then spread into a tow and oxidized in ovens. Finally, the fibers go through the final step in the process called carbonization. In this step, the fibers go through a series of ovens in an oxygen-free environment to remove non-carbon molecules, producing fibers that are typically over 90 percent carbon [19]. Once the fibers are finished, surface treatments or sizing can be added to improve fiber properties or encourage adhesion based on the fiber's intended use.

The first type of carbon fiber used in this research was Hercules AS4. According to the manufacturer, the AS4 fiber has a tensile strength of 4.43 GPA, a tensile modulus of 231 GPA, and an average diameter of 7.1 μm [13]. These fibers have been electrochemically oxidized and have a proprietary surface treatment to increase their ability to bond with an epoxy [5]. SEM measurements of the diameter of the fibers ranged from 6.7-8.2 μm, which agree with the average diameter given by the manufacturer. The second fiber type used was Thornel T650 fibers (Cytec). Properties of the T650 fiber include a tensile strength of 4.28 GPa, tensile modulus of 255 GPa, and an average diameter of 6.8 μm. These fibers have been sized with a 1% UC.309 epoxy sizing [20]. Measurements of the diameter taken using the SEM ranged from 6.7-7.2 μm, which again agree with the average diameter given by the manufacturer. Both the AS4 and the T650 fibers came in a 6K tow and were used as received by the suppliers. As an example of the fiber tows and the diameter measurement technique, the T650 carbon fiber tow and SEM measurements of a T650 fiber are shown in Figure 3.1 and Figure 3.2, respectively.

Figure 3.1 6K T650 carbon fiber tow

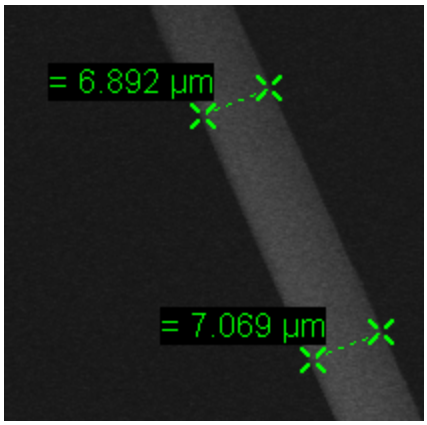

Figure 3.2 SEM measurement of T650 fiber diameter

Two matrix materials were used in this research. Both materials have properties that make them well-suited for use in the aerospace industry [21, 22]. The first matrix used was Epon828 epoxy resin. Epon828 is a difunctional bisphenol A/epichlorohydrin derived resin that can be mixed with different curing agents to obtain excellent mechanical, chemical resistance, adhesive, and dielectric properties [21]. Its versatility makes it useful for not only the aerospace industry, but for marine coatings, tooling, and electrical and chemical applications among others [21]. For this research, the Bisphenol A diglycidyl ether was mixed with a diethylenetriamine hardener in a 100:12 weight ratio (Sigma-Aldrich). The second matrix used was Cycom 5320-1 (Cytec). Cycom 5320-1 was specially designed for out-of-autoclave manufacturing applications. It can be cured at low temperatures, which makes it useful for prototyping as well [22]. This matrix was provided in B-stage film form. B-stage resin is partially cured, and the film sheets had to be frozen until used as the epoxy will continue to cure at room temperature.

Specimen Preparation

Three different fiber/matrix combinations were studied. The material systems used were AS4/Epon828, T650/Epon828, and T650/Cycom 5320-1. A description of how specimens for each material system were made follows in this section, but a more detailed, step-by-step process is included in Appendix A.

AS-4/Epon828 and T650/Epon828

To make specimens using the Epon828 epoxy, fibers were first suspended across a circular void (diameter of 2 cm) in a metal plate and secured on either side with double-sided

tape. Then the Epon828 was prepared. This was done by first placing a clean plastic cup on a high resolution scale (Explorer Pro analytical balance from OHAUS). The scale was then zeroed and 3-5g of bisphenol A diglycidyl ether was added to the cup. The diethylenetriamine hardener was then added in the proper weight ratio, with the scale measuring the respective weights of the materials. The mixture was then stirred for several minutes with a glass rod until many small air bubbles were visible in the epoxy, ensuring the material was thoroughly mixed. The epoxy was then allowed to sit for several minutes until the air bubbles were no longer present. Droplets were formed within 30 minutes of mixing the Epon828 as the epoxy cures at room temperature in large enough quantities, and the matrix became less viscous and more difficult to work with after that amount of time. Epoxy droplets were deposited on the fiber using a small wire sanded to a fine tip. The wire was dipped into the epoxy, and a large drop of the matrix was swiped along the fiber. Many smaller droplets (10 μm ≤ d ≤ 300 μm) were formed on the fiber using this method. In order to test the droplets later, there needed to be at least 1.2 mm between them for the knife edges, so the unwanted droplets were removed from the fiber using the same wire. Droplets were selected to keep based on their size and location. On average, four droplets with diameters in the range of 30 μm-130 μm separated by several millimeters were kept on each fiber. Figure 3.3 shows a portion of a fiber after droplets were deposited, but before the unwanted droplets were removed. The selection process to determine which droplets needed to be removed is shown briefly as well.

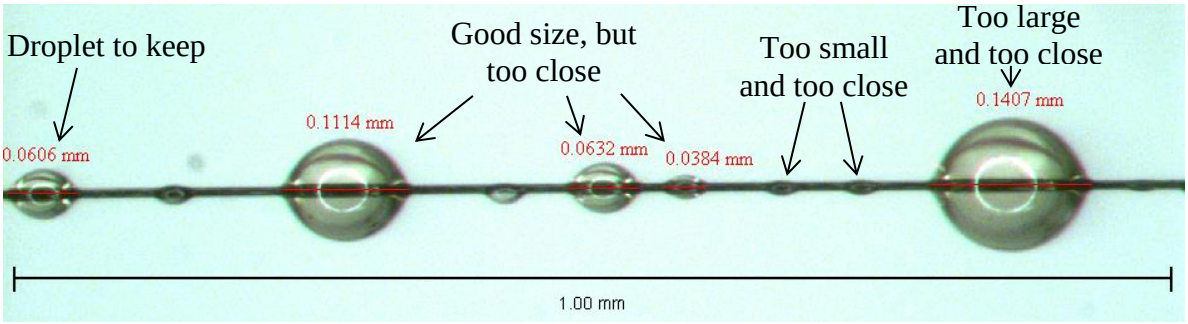

Figure 3.3 Part of a typical fiber after the large drop of epoxy was swept across it and formed droplets, but before unwanted droplets were removed.

Once the specimens were prepared, they were then cured in an oven using one of the cure cycles listed in Table 3.1. A description of the first cure cycle follows, and each cycle was

carried out in a similar way with their respective times and temperatures. For the first cure cycle, the droplets were placed in an oven (VersaTenn III from Tenney Environmental), which was preheated to 80°C. After two hours, the oven was turned up to 150°C. Two hours later, the oven was turned off, and the specimens were left in the oven to cool overnight. The specimens were allowed to slowly cool with the oven in an effort to reduce potential residual stresses caused by a difference in thermal expansion coefficients between the fiber and epoxy. It should be noted that for the Epon828 epoxy system, cure cycles 1, 5, 6, and 7 were taken from references [18], [11], [11] and [12], respectively. Typical cured Epon828 droplets on both fiber types are shown in Figure 3.4.

Table 3.1 Cure cycles used for AS-4/Epon828 and T650/Epon828 specimens

Cure Cycle
1: 2hr@80°C, 2hr@150°C
2: 2hr@80°C, 2.5hr@150°C
3: 2hr@80°C, 3hr@150°C
4: 2hr@80°C, 4hr@150°C
5: 2hr@60°C, 1hr@120°C, 5hr@180°C
6: 24hr@60°C
7: 2hr@90°C, 1hr@120°C

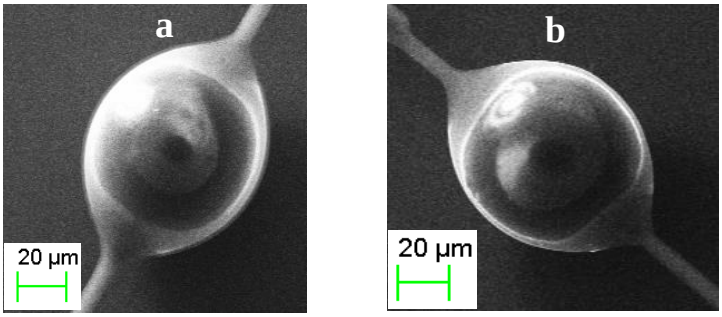

Figure 3.4 Typical Epon828 droplets (a) on AS-4 fiber and (b) on T650 fiber

T650/Cycom 5320-1

The Cycom 5320-1 was provided in B-stage film form, so droplet formation was more difficult with this resin. In order to make the T650/Cycom 5320-1 specimens, a small amount of resin film was taken from the freezer and placed on a glass microscope slide in an aluminum foil boat. Fibers were suspended across a plate in the same manner as described previously. The foil

boat and the plate with the fibers were then placed on a hot plate set to 120°C. The foil boat was put on the hot plate in order to make the resin viscous enough to work with. The plate with the fibers was put on the hot plate in an effort to heat the fibers so the matrix did not cool immediately upon contact. This temperature was chosen as it is the first temperature in one of the manufacturer's recommended cure cycles for the matrix (3 hours at 121°C, followed by 2 hours at 177°C) [22]. Once the matrix was viscous enough, a wire was used to transfer resin from the glass plate to the fibers. This process was difficult as the matrix cooled some in the transition. Some excess droplets were removed from the fibers, but the droplets cooled quickly on the fibers, and if not removed immediately, became too sticky to be successfully removed. Once the specimens were complete, they were placed in an oven preheated to 121°C for the remainder of the three hours in the first step of the cure cycle. The oven was then turned up to 177°C and was shut off two hours after the temperature was increased. Again, the specimens cooled in the oven overnight. A typical Cycom 5320-1 droplet is shown in Figure 3.5.

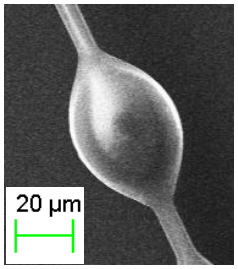

Figure 3.5 Typical T650/Cycom 5320-1 specimen

Chapter 4 - Experimental Procedures

Before the specimens were tested, the embedded length of the fiber in each droplet was measured and recorded, and the location of each droplet on the fiber was noted. Several measurements were taken of each droplet, and the average of those measurements was recorded as the embedded length. This was done using an Olympus SZH10 stereoscopic microscope equipped with a Spot Insight digital camera producing a maximum combined magnification of 140X [2]. As mentioned in the previous chapter, fiber diameter was taken from the manufacturer's data sheet and verified using SEM measurements. Using the embedded length measurements and the fiber diameter values, the embedded area for each specimen was then calculated. The specimens were also analyzed to look for any imperfections and to note the general shape of each droplet. Droplets with imperfections would not be tested.

The shape of the droplets varied slightly. Some were spherical, others elliptical, but most were a combination, being more spherical with a meniscus on either side. Examples of the different droplet shapes are shown in Figure 4.1. Measurements of the embedded lengths of droplets are also shown in Figure 4.1. The mostly spherical droplet with a small meniscus on either side (shown in Figure 4.1b) is what typically formed on fibers in this study. Although this was not always the case, it was noted that generally the larger the embedded length, the more spherical the droplet was. Figure 4.1b and c show this relationship, but Figure 4.1a is an exception and is more elliptical. The typical droplet shape was consistent with droplet shapes reported in other studies that used similar epoxy matrices [23, 10, 11, 12]. Kang et al [10] also note that the meniscus is about the same size regardless of embedded length, so it is a smaller portion of the larger droplet than the smaller droplet. This means that larger droplets will usually be more spherical than smaller ones [10].

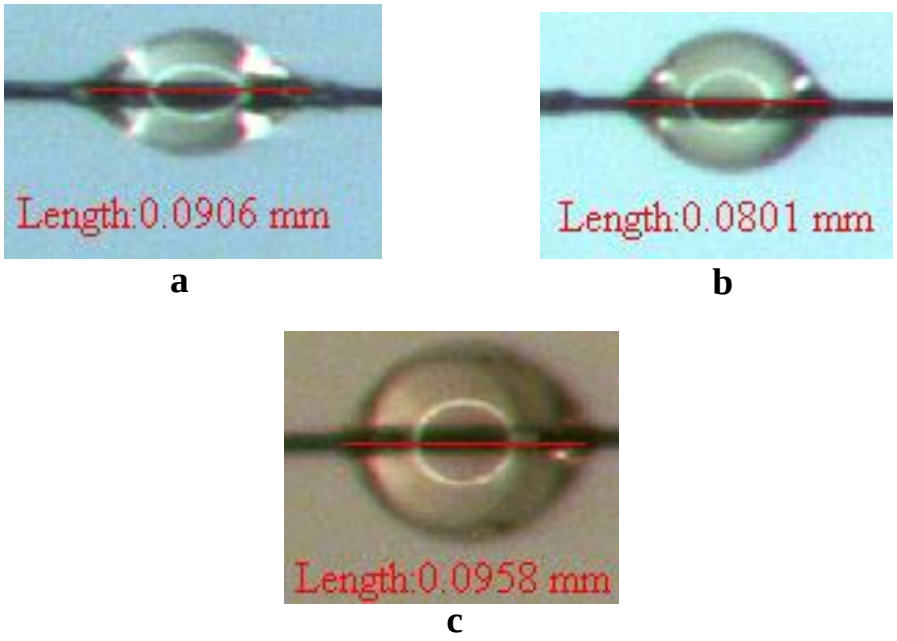

a **b**

c

Figure 4.1 Examples of droplet shapes: (a) more elliptical (b) typical droplet shape (c) more spherical

The microbond testing device was developed by another graduate student in the same research group, and is shown in Figure 4.2 [2]. The main components of the device are the motorized stage, the 1N load cell, the movable knife edges, and the tabs to support the fiber. Figure 4.2 (a) shows a front view of the test device with the load cell and stages shown. Figure 4.2 (b) is a close-up of the top view of the device with a specimen on the support tabs and the knife edges in place ready for testing. Not shown in the figure is an optical microscope placed above the testing device to help align the fibers and knife edges and observe the specimen during testing. The load cell is connected to a force transducer (Interface 9320-2 TEDS), which is in turn connected to a computer. A data acquisition program was written in MatLab to record the time and force data from each test. Data was recorded three times every second.

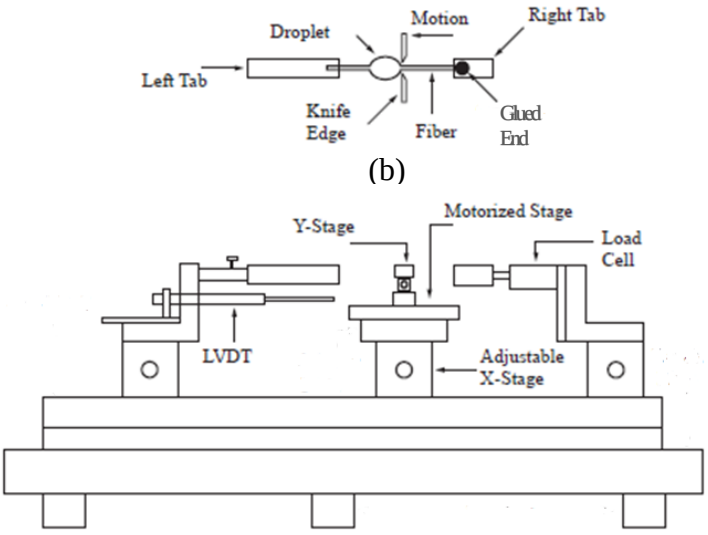

Figure 4.2 Microbond Testing Device. (a) Front view of the microbond testing device. (b) Close-up of top view of testing device with specimen and knife edges in place for testing.

For the microbond test, a fiber was carefully taken from the metal plate and suspended across the gap between the left and right tabs on the testing device (see Figure 4.2 (b)). This was done using tweezers to break the fiber where it attached to the tape on both ends and carefully transferring it so it rested on the left and right tabs. This process was difficult as it was easy to break a fiber during transfer if gripped too tight, usually rendering it unusable, or dropping it if not gripped tight enough. The gap between the tabs varied from about 7-15 mm, depending on the fiber length and position of the droplets. The left tab was moved to support the fiber approximately 3 mm to the left of the droplet closest to it. The fiber was aligned as parallel with the tab edges as possible to avoid any bending in the glued end of the fiber during testing. Once it was properly aligned, the fiber was glued to the right tab using Loctite380 Instant Adhesive with Loctite7113 Accelerator (R.S. Hughes). The specimen was left for at least 10 minutes to allow the adhesive to harden. Once the fiber was secured, the adjustable x-stage was moved so the knife edges were close to the droplet, between it and the right tab. The knife edges were then carefully adjusted so the distance between them was greater than the diameter of the fiber, but less than that of the droplet. First, one knife edge was brought in contact with the fiber and the x-stage was moved so the knife edge was close to the droplet, but not touching it. Next, the second knife edge was adjusted until it looked as if it was about to touch the fiber. Finally, a

small hand-held microscope was used to look at the setup from the side, and the knife edges were then moved closer together until the tiniest sliver of light could still be seen between them. This method usually resulted in normal tests, which meant the knife edges were properly adjusted to have a gap larger than the fiber diameter, but smaller than the droplet diameter. Occasionally for smaller droplets, this method would not result in a test as the knife edges did not get close enough together to contact the droplet. If this happened, the process was repeated, but the knife edges were brought closer until less or no light was visible between them and normal data was obtained.

Aligning the knife edges was a challenging process for several reasons. The knife edges were very large compared to the droplet and fiber, and the edges were difficult to see well when the microscope was focused on the droplet. Also, there was a learning curve to get used to the knife edge adjustments. In several of the first tests run with this device, the knife edges were moved too quickly or there wasn't enough experience to know when they were close enough and the second knife edge would also contact the fiber. This was not desirable as squeezing the fiber between the knife edges potentially damaged the fiber and resulted in fiber failure instead of debonding.

Once the knife edges were in place, the data acquisition software was started. The motorized stage was then immediately started in motion toward the droplet (away from the load cell) at a rate of 0.12 mm/min (0.002 mm/s). This rate was chosen as it was used for microbond tests by another student in the research group [2] and is a value in the range of 0.05 mm/min - 1.0 mm/min used by others [10, 11, 12, 18, 24, 25]. The motor and data acquisition were stopped when failure of either the droplet or the fiber occurred.

The raw data recorded from the tests consisted of force (N) and time (s). The data was analyzed using Microsoft Excel 2010. Data analysis consisted of converting time to displacement by multiplying the time value by the crosshead speed. Also, the force data was adjusted so the initial force reading was zero for each test if necessary. A graph of Force vs. Time was made and any unnecessary data before the knife edges contacted the droplet or after failure occurred was removed. A typical Force vs. Displacement graph is shown in Figure 4.3.

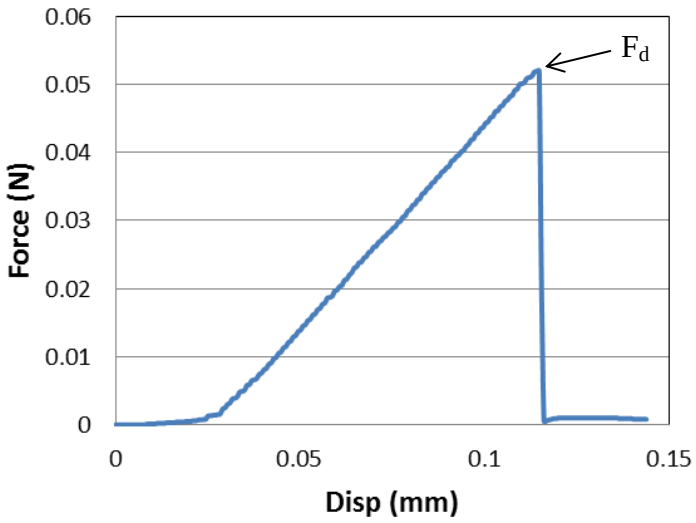

Figure 4.3 Typical Force vs. Displacement graph obtained from data analysis

The graphs typically have four main sections: droplet deformation, loading, debonding, and post-test. The droplet deformation section is the gradual increase of force from the beginning of the graph where the knife edges contacted the droplet until the slope of the graph becomes constant (approximately 0.0 mm-0.03 mm for the test shown in Figure 4.3). Although cured, the droplets likely deform slightly as the force of the knife edges increases, causing this initial gradual increase in force [11]. The graph shown is from an AS4/Epon828 specimen with Cure1. The droplet deformation section on the graphs from specimens with longer cure times tends to be smaller. This is likely due to the droplets achieving a higher level of cure and not deforming as much. Once the force becomes great enough, the droplet no longer deforms, and the slope increases rapidly and is relatively constant. This is the loading section (approximately 0.03 mm-0.12 mm for the test shown). Once the force of the knife edges on the droplet exceeds the strength of the bond between the fiber and droplet, the droplet shears (debonds) from the fiber, and the force drops drastically (approximately 0.12 mm for the test shown). After debonding, the droplet slides along the fiber until the test is stopped. This can be seen in the post-test portion of the graph (approximately 0.12-0.14 mm for the test shown). In most cases, little to no friction registers on the graph. A very small amount of friction can be seen in the graph shown. In tests where the fiber broke, the force in the post-test portion of the graphs was zero as the fiber was no longer there.

After testing was complete, the interfacial shear strength, τ_{IFSS}, was calculated using Eq. (2) (originally shown in Ch2, but repeated here for convenience),

$$\tau_{IFSS} = \frac{F_d}{\pi d l_e} \qquad (2)$$

where max force, $F_{d,}$ was as defined in Figure 4.3, embedded length, l_e, was as defined in Figure 4.1, and fiber diameter, d, was used as given by the manufacturers.

Chapter 5 - Experimental Results and Discussion

This chapter contains the actual results obtained from the microbond tests performed in this study as well as discussion of these results and comparison to results from other researchers.

Experimental Results

AS4/Epon828

Of the three material systems used in this research, the AS4/Epon828 was tested most extensively and the results for this system will be presented first. The first tests run were with various cure cycles used by others. These tests were run simply to ensure that the tests were performed properly and results could be obtained that were similar to those found by others. The initial cure cycles used are shown in Table 5.1.

Table 5.1 Comparison of results found with the current research with those found by others using different cure cycles

		Reference's Data		Current data	
Reference	Cure Cycle	Material System	$\tau_{IFSS(avg)}$ (MPa)	Material System	$\tau_{IFSS(avg)}$ (MPa)
11	2hr@60°C, 1hr@120°C, 5hr@180°C	T-300/Epon828	50.2	AS4/Epon828	50.4
12	2hr@60°C, 1hr@120°C, 5hr@180°C	AS4/Epon828	77.7	AS4/Epon828	50.4
18	2hr@80°C, 2hr@150°C	Celion carbon fiber/Epon828	65.3	AS4/Epon828	27.5
11	24hr@60°C	T-300/Epon828	44.2	AS4/Epon828	N/A
12	2hr@90°C, 1hr@120°C	T300/Epon828	72.3	AS4/Epon828	N/A

The data from Biro et al. (1991) [11] matched very well with that from this research. The overall trends of the Force vs. Embedded Area and Force vs. Embedded Length graphs were very similar as well. This was very encouraging and suggested that the test method was being carried out properly in the current research. The system used by Biro et al. (1993) was the most similar to that used in this research, but the interfacial shear strength values differed by almost 30 MPa. The majority of the difference is probably due to the fact that this research used a diethylenetriamine hardener in the Epon828, oven to cure, and a slower cure rate of 0.12

mm/min, while Biro et al. (1993) used a Tonox hardener, nitrogen in a Lindberg tube furnace to cure, and a faster test rate of 2 mm/min [12]. Even though the final numbers differed, the overall trends from the force vs. time graphs were similar. These same variations in hardener and test parameters were used in the experiments from Biro et al. (1991) [11], but the difference in fiber types might have inadvertently caused the data to line up better with the current research. The interfacial shear strength value from Gaur [18] is more than double that from the same cure cycle used in this research, but again, difference in personnel, fiber type, hardener, and test rate were probably responsible for most of that difference. The results from the last two cure cycles in Table 5.1 are not comparable since those cure cycles did not cure the epoxy used in this research enough to test. The results from the initial tests in this study were close enough those found by others to confirm the method used in this research was being performed properly and other cure cycles could be tested confidently.

Once it was determined the microbond test could be performed successfully, the cure cycle from [18] was strategically changed in order to determine the effect cure time had on the IFSS. This cure cycle was chosen since it was fairly simple, consisting of just two steps, and the preliminary data looked the best out of the four cure cycles used in the evaluation stage that was just discussed. The variations of the cure cycle are shown in Table 5.2. In this paper, the cure cycles will be referred to as Cure1, Cure2, etc. according to the numbering in the table. They are numbered based on the time of final cure, but will be discussed chronologically in the order in which they were tested.

Table 5.2 Variations of cure cycles used in this research

Cure Cycle	Cure times
1	2hr@80°C, 2hr@150°C
2	2hr@80°C, 2.5hr@150°C
3	2hr@80°C, 3hr@150°C
4	2hr@80°C, 4hr@150°C

Cure1 was performed first as it was one of the cure cycles used in the original experiments (cure cycle from [18] in Table 5.1). For this cure cycle, 30 total tests were run, where 27 were successful debonding tests and three were fiber breaks. The Force vs. Embedded

Length (L_e) and Force vs. Embedded Area (A_e) graphs for this test are shown in Figure 5.1a and Figure 5.1b, respectively. (Fiber breaks are not represented on the graphs.)

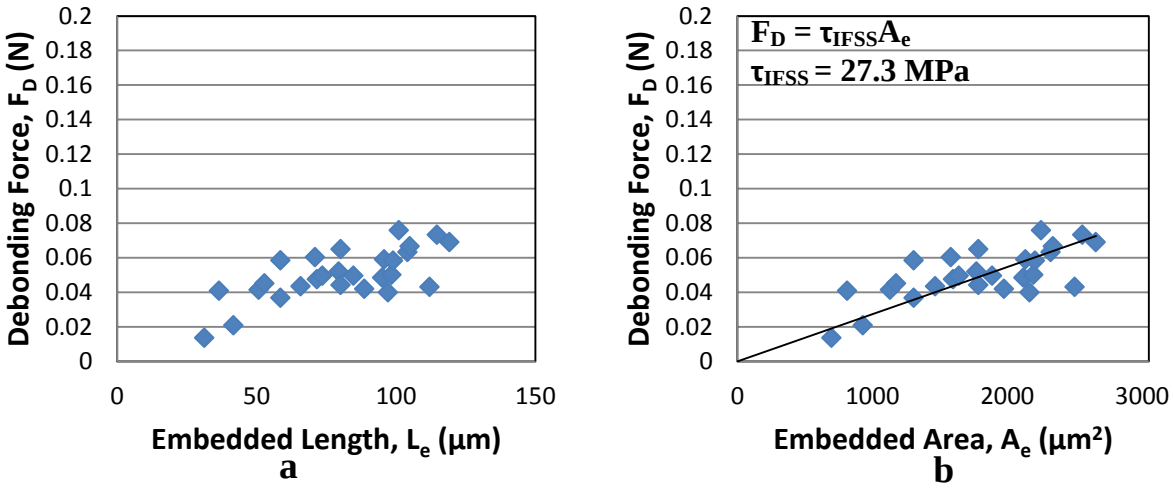

Figure 5.1 Graphs for AS4/Epon828 system cured with Cure1. (a) Force vs. L_e, and (b) Force vs. A_e with regression analysis

The data from Cure1 (shown in Figure 5.1a and Figure 5.1b) shows an upward linear trend and lines up fairly well with the origin, but it also has a decent amount of scatter. The IFSS found by averaging the values from Eq. (2) was 29.1 MPa, which matches well to 27.3 MPa from the Force vs. Area graph in Figure 5.1b.

While the droplets in Cure1 were cured enough to test, it did not seem as though they were fully cured. The droplets kept their shape and were hard enough to test, but seemed a little tacky after testing. Other cure cycles in Table 5.1 with higher times and temperatures gave higher IFSS values, which also contributed to conclusion that the Cure1 droplets were not fully cured. Also, it looked as if lower cure times or temperatures would not cure the epoxy enough to test based on the lack of testable specimens from the last two of the initial cure cycles listed in Table 5.1. The logical choice for incrementing time of cure was then to increase the amount of time for the final cure. Since it was not known how much of an increase of time would be necessary to produce a noticeable change in IFSS for this material system, it was decided to double the time of the final cure to four hours for the next cycle (Cure4). A total of 33 tests were run with Cure4, where 16 were successful debonding tests, and 17 were tests in which the fiber broke. The Force vs. Embedded Length and Force vs. Embedded Area graphs for this cure cycle are shown in Figure 5.2a and Figure 5.2b, respectively.

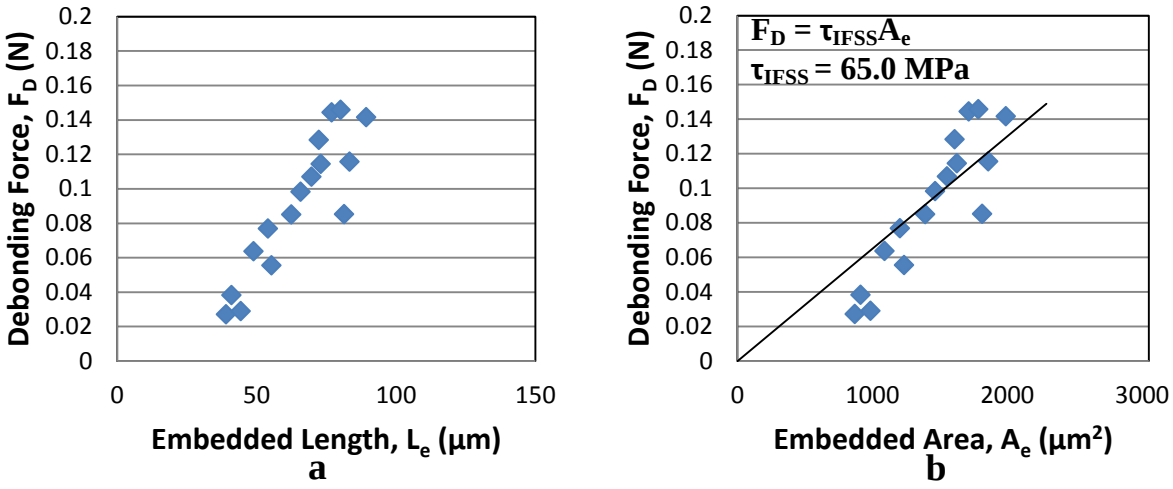

Figure 5.2 Graphs for AS4/Epon828 system cured with Cure4. (a) Force vs. L_e, and (b) Force vs. A_e with regression analysis

As expected (based on results from Biro et al. (1991) [11]), droplets from Cure4 were bonded much more strongly to the fiber than droplets from Cure1. The largest force value obtained using Cure1 was 0.069N, while that from Cure4 was 0.142N. Perhaps a better comparison of the change in bond strength is that for the same sized droplet, Cure1 had a debonding force of 0.0434N, while Cure4 has a debonding force of 0.098N. Another point of discussion is the range of embedded lengths tests. Embedded lengths of up to 120 μm could be tested with the shorter time in Cure1, while the largest testable embedded length for Cure4 was about 90 μm. Beyond this value, the fiber broke during the test. The stronger bonding and higher values of force indicated that a higher level of cure had been achieved.

The data from Cure4 is linear, but has a decent amount of scatter and does not line up as well with the origin, as seen in the regression analysis. The stray from the origin is also indicated by comparing the IFSS values from the average of the raw data and from the regression analysis. The former gave a value of 60.1 MPa, while the latter gave a value of 65.0 MPa. These are still relatively close, but do not match as well as those from Cure1 where the regression line fit the data much better. The lower values for the smaller embedded lengths resemble the results from Kang et al. [10] discussed in Chapter 2.

Since the IFSS from Cure4 was significantly higher than that from Cure1 and it was not possible to test droplets with large embedded lengths due to fiber failure, a level of cure between the two was desired. Therefore the next cure cycle, Cure3, had a final cure time of three hours.

With this cure cycle, 36 total tests were run, where 27 were successful debonding tests and nine were fiber breaks. The Force vs. Embedded Length and Force vs. Embedded Area graphs from the successful tests are shown in Figure 5.3a and Figure 5.3b, respectively.

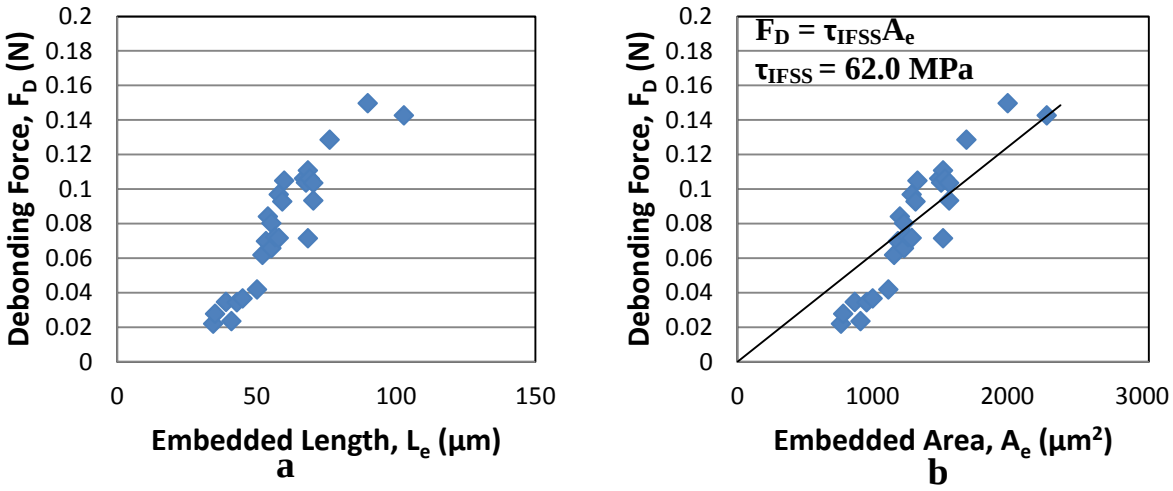

Figure 5.3 Graphs for AS4/Epon828 system cured with Cure3. (a) Force vs. L_e, and (b) Force vs. A_e with regression analysis

The data from Cure3 has slightly less scatter and lines up better with the origin than Cure4. The IFSS found by averaging values from Eq. (2) was 57.0 MPa, while the regression analysis gave a value of 62.0 MPa. These numbers are only a few MPa lower than Cure4, meaning that with a final cure time of three hours, the epoxy reached essentially the same level of cure as it did with a longer cure time of four hours.

In hopes of finding a level of cure between Cure1 and Cure3, Cure2 was used for another set of specimens. This cure cycle had a final cure time of 2.5 hours. A total of 26 tests were run with this cure cycle, where 20 were successful debonding tests, and six were fiber breaks. The results of the successful tests are shown in the Force vs. Embedded Length and Force vs. Embedded Area graphs in Figure 5.4a and Figure 5.4b, respectively.

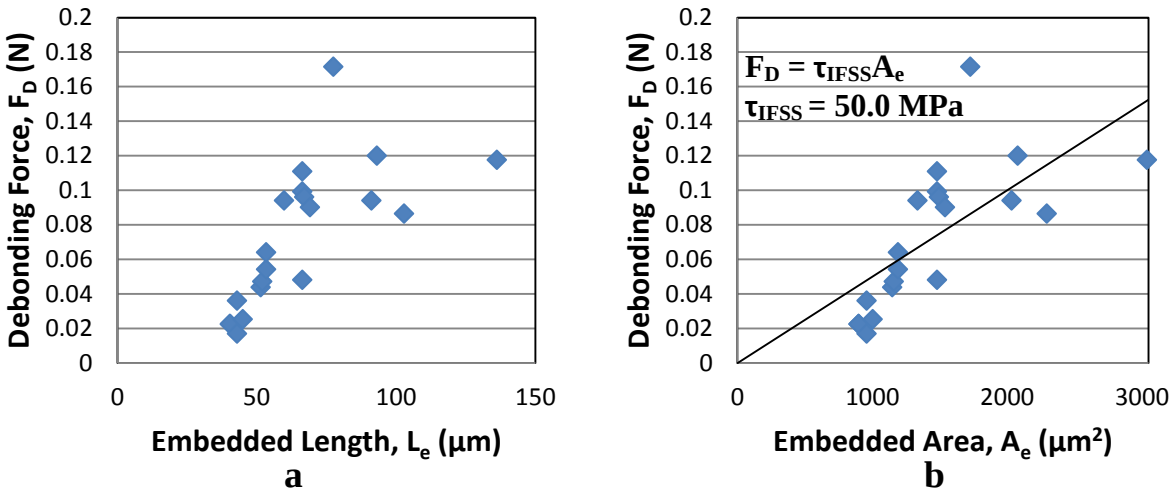

Figure 5.4 Graphs for AS4/Epon828 system cured with Cure2. (a) Force vs. L_e, and (b) Force vs. A_e with regression analysis

The data from Cure2 has the most scatter of any of the cure cycles looked at. Within its scatter band, it lines up with the origin better than Cure3 and Cure4, however. The IFSS found from Eq. (2) was 47.8 MPa, while the regression analysis gave a value of 50.0 MPa. These numbers are in between those from Cure1 and Cure3, but are closer to Cure3. This shows that full cure can be achieved with a final cure time of about three hours at a temperature of 150°C when first cured at 80°C for two hours. Any additional final cure time does not increase the strength of the bond between the materials.

T650/Epon828

The preliminary comparative cure cycles in Table 5.1 were not run with the T650/Epon828 specimens as the T650 fibers did not arrive until after those preliminary tests were finished. Also, it did not seem necessary to run those tests with the T650 since those were run simply to ensure the microbond test could be carried out successfully. Once the fibers arrived, the same four cure cycles listed in Table 5.2 were used for T650/Epon828 specimens. The data will be presented in the same order as the AS4/Epon828 specimens: Cure1, Cure4, Cure3, Cure2. Data will be presented and comparisons to other T650/Epon828 cure cycles will be made here. A discussion about how T650 data compares to AS4 data will be conducted after the data is presented. Outside research of testing T650 fibers with the microbond method was not found, so no comparisons between data from this research and that from others could be

made. For this material system cured with Cure1, 50 total tests were run, with 49 successful debonding tests, and only one fiber break. Force vs. Embedded Length and Force vs. Embedded Area graphs for the T650/Epon828 system using Cure1 are shown in Figure 5.5a and Figure 5.5b, respectively.

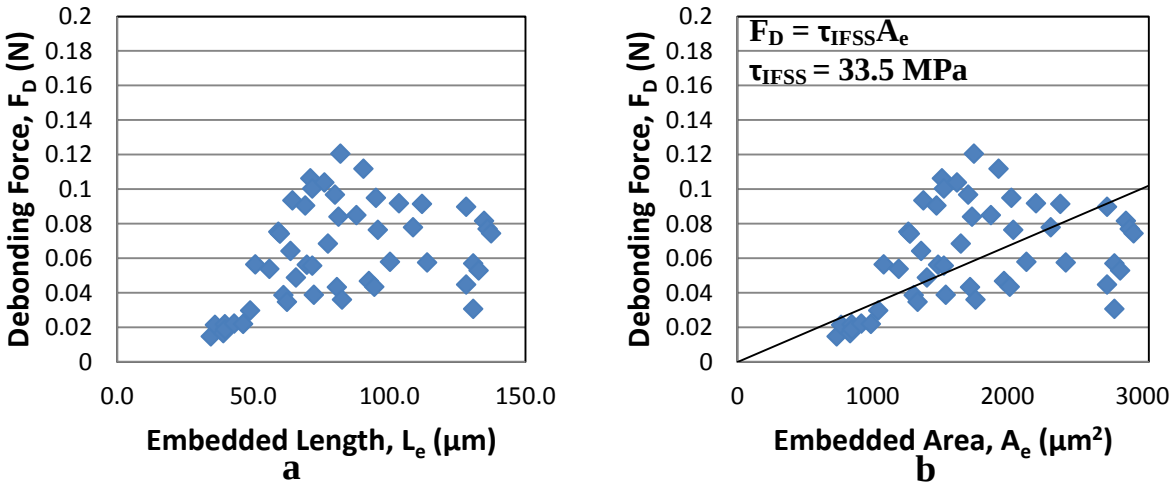

Figure 5.5 Graphs for T650/Epon828 system cured with Cure1. (a) Force vs. L_e, and (b) Force vs. A_e with regression analysis

This data has a significant amount of scatter, especially beyond about 1200 μm^2. With so much scatter, it is difficult to say whether the data lines up well with the origin or not. There seem to be a few more data points above the regression line than below, but the IFSS value from the calculations still matches fairly well with the regression analysis. The former gave a value of 36.9 MPa, while the latter gave a value of 33.5 MPa. Compared to the same cure cycle used with the AS4/Epon828 specimens, the T650/Epon828 specimens were about 7 MPa stronger.

As with the previous material system, the Epon828 droplets on the T650 fibers cure with Cure1 seemed a little tacky as if the matrix was not cured completely. The less cured state of the matrix is likely responsible for much of the scatter for Cure1 in both material systems. The droplets probably start curing on the outside first, and although minimal, some curing possibly occurs inside next to the fiber as well as the fiber heats up. The matrix from the mid-diameter region and toward the fiber would be the last to cure. This would explain why the droplets were cured enough to test, but were tacky afterward since the droplets likely deform during testing, and without being fully cured, would not return to their original shape after debonding. Droplets

with different shapes would achieve different levels of cure. An elliptical droplet would likely have a larger majority of the droplet cured than a spherical droplet with the same embedded length. With more of its matrix cured, the elliptical droplet would then show a higher IFSS during testing. Therefore, different shaped droplets with varying levels of cure would contribute to scatter in the data.

The next cure cycle used with this system was again Cure4. With this cure cycle, 29 tests were run, where 16 were successful debonding tests and 13 were fiber breaks. Force vs. Embedded Length and Force vs. Embedded Area graphs from Cure4 are shown in Figure 5.6a and Figure 5.6b, respectively.

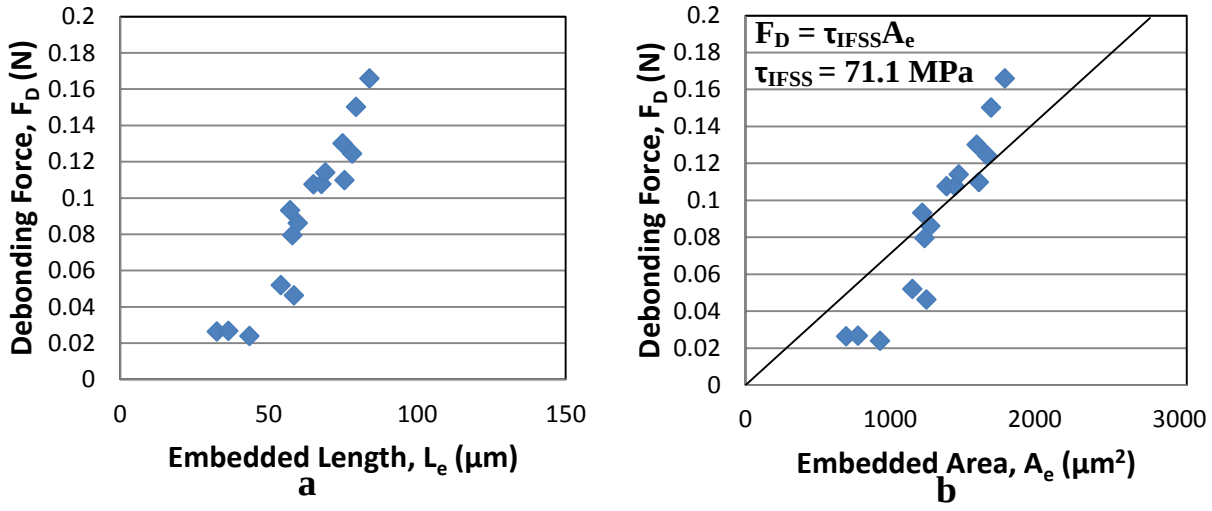

Figure 5.6 Graphs for T650/Epon828 system cured with Cure4. (a) Force vs. L_e, and (b) Force vs. A_e with regression analysis

The data from Cure4 is much cleaner and has less scatter than Cure1. It also shows an upward linear trend, but the trend is a little steep to line up with the origin. This is most likely due to the epoxy being cured to a higher degree with the longer time in the oven. The IFSS found by averaging values calculated using Eq. (2) was 63.7 MPa, which is further from the regression analysis value of 71.1 MPa than desired, but is still acceptable.

Cure3, with a final cure time of three hours was used next. A total of 36 tests were run, where 27 were successful debonding tests, and 9 were fiber breaks. Force vs. Embedded Length

and Force vs. Embedded Area graphs from Cure3 are shown in Figure 5.7a and Figure 5.7b, respectively.

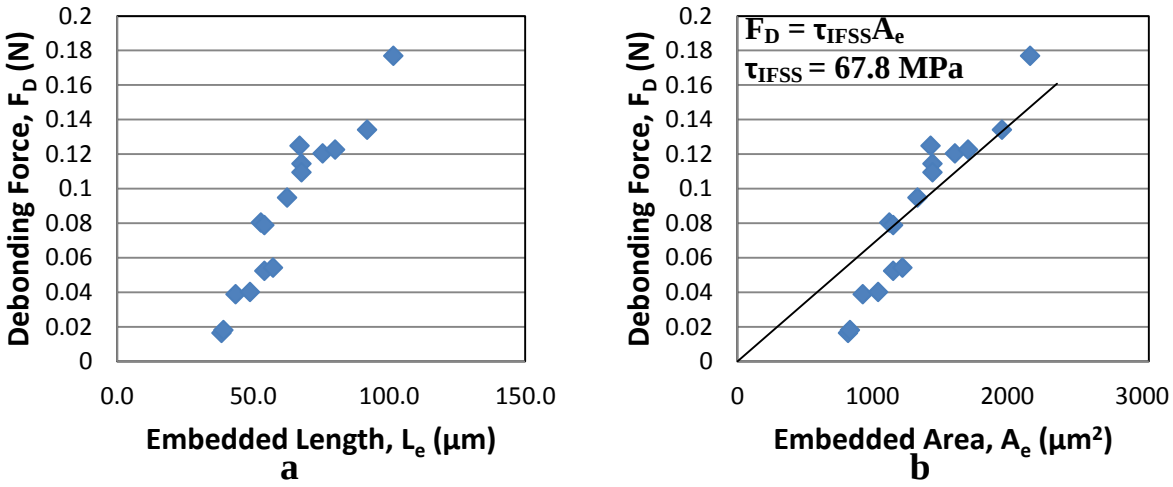

Figure 5.7 Graphs for T650/Epon828 system cured with Cure3. (a) Force vs. L_e, and (b) Force vs. A_e with regression analysis

The data points from Cure3 show a fairly upward linear trend. While the linear trend is a little steep and doesn't line up with the origin, the data itself looks relatively tight without much scatter. The analysis using Eq. (2) gave an IFSS value of 59.7 MPa, while the regression analysis gave a higher value of 67.8 MPa as shown in Figure 5.7b. As with Cure4, the difference between these two values is approximately 8 MPa, which is higher than desired, but still seems acceptable.

The final cure cycle run with this material system was Cure2, with a final cure time of 2.5 hours. Again, this cure cycle was used in hopes to achieve a level of cure between Cure1 and Cure3. Based on the results from the AS4/Epon828 material system, the results for this cure cycle were expected to be slightly lower than those from Cure3. A total of 28 tests were run, where 24 were successful debonding tests and six were fiber breaks. The Force vs. Embedded Length and Force vs. Embedded Area graphs for Cure2 with the T650/Epon828 material system are shown in Figure 5.8a and Figure 5.8b, respectively.

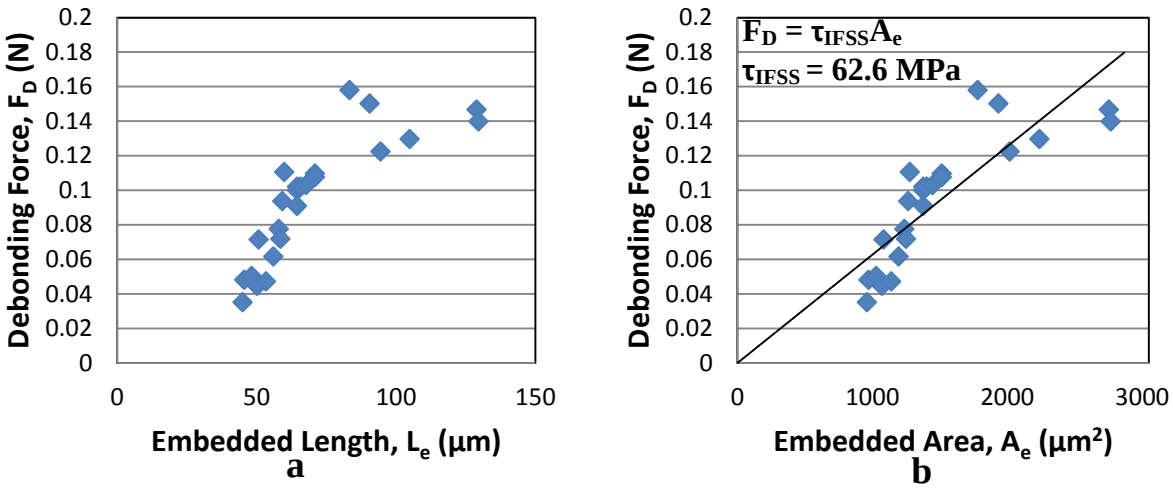

Figure 5.8 Graphs for T650/Epon828 system cured with Cure2. (a) Force vs. L_e, and (b) Force vs. A_e with regression analysis

Cure2 has interesting data. From 45-70 µm, the data is tight without much scatter. Beyond 70 µm, however, the data seems to level off and shows considerably more scatter. Although it doesn't look like the data lines up very well with the origin, the IFSS found using the average of the values from Eq. (2) and the regression analysis are both 62.6 MPa. As expected, this value is between those from Cure1 and Cure3, but is closer to Cure3.

Carbon fiber/Epon828 Results Discussion

The results from both the AS4/Epon828 and T650/Epon828 material systems were quite similar for corresponding cure cycles. Both showed low IFSS with a shorter final cure time. The IFSS increased as final cure time increased, although from Cure3 to Cure4, the increase was minimal. This can be seen in Figure 5.9a and Figure 5.9b, which show the average IFSS along with error bars for standard deviation for the AS4/Epon828 and T650/Epon828 material systems. A longer final cure would likely not produce a higher IFSS, indicating that the matrix was fully cured at that point.

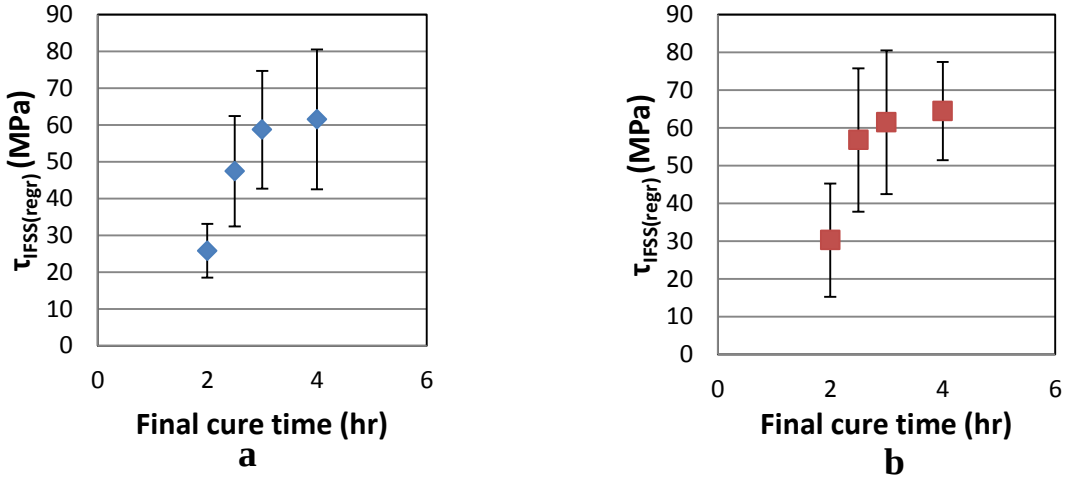

Figure 5.9 Graphs summarizing IFSS values from all cure cycles. (a) AS4/Epon828 and (b) T650/Epon828 material systems

Figure 5.10 makes it a little easier to compare the two material systems. This figure shows that both material systems follow the same trend, with the T650/Epon8282 system having slightly higher values for all cure cycles. The main difference is seen in Cure2 (2.5 hr final cure time), where the systems differed by about 10 MPa. This shows that the T650/Epon828 system reached a higher level of cure at that point, and overall probably reaches its fully cured state with a shorter final cure time than the AS4/Epon828 system would require.

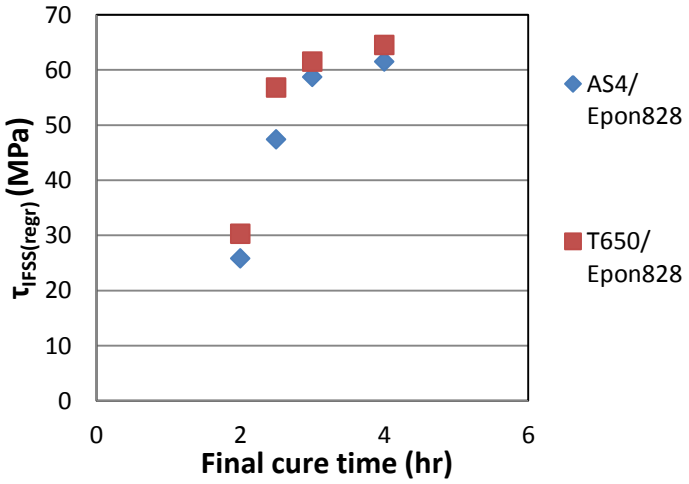

Figure 5.10 Graph of IFSS vs. Final cure time for both AS4/Epon828 and T650/Epon828 material systems

The increase in IFSS with the increase in the time of cure could mostly be explained by the nature of the bond between the two materials. The factors that influence IFSS were discussed in Chapter 2, but will be briefly discussed here again. The adhesion between the materials in a composite is a combination of physical, mechanical, and chemical factors. The mechanical factor is basically mechanical interlocking between the two materials. The carbon fibers are not perfectly smooth, so the wet epoxy can fill any grooves or imperfections in the fiber. Once cured, the hardened epoxy then has to overcome being physically intertwined with the fiber before the droplet will move during testing. The mechanical component is affected by changes in cure cycle in a more secondary nature than the physical and chemical factors. The physical and chemical interactions consist of van der Waals interactions and possibly covalent bonds [11, 12]. As the matrix cures, the heat affects the bonds, and cross-linking occurs. Higher temperature leads to more cross-linking, which leads to a more cured, and more stable matrix [2, 25]. With a more cured matrix, the mechanical interactions would be more difficult to overcome since the epoxy would be harder and less likely to deform. All of these factors together help the IFSS increase with an increase in the time and/or temperature of the cure cycle.

T650/Cycom 5320-1

The T650/Cycom 5320-1 material system was not cured with the same cure cycles as the previous material systems since the matrix material was different (Cycom 5320-1 instead of Epon828). Two cure cycles were suggested by the manufacturer [22] to fully cure the Cycom 5320-1 matrix, and they are listed in Table 5.3.

Table 5.3 Cure cycles suggested by the manufacturer and used for T650/Cycom 5320-1 material system [22]

Cure Cycle	Cure times
A	3hr@121°C, 2hr@177°C
B	12hr@93°C, 2hr@177°C

These cure cycles differ from those used for the Epon828 specimens. In Cure1 - Cure4, only the final cure time changed, but in CureA and CureB, the time and temperature of the initial cure cycle are significantly different, while the final cure time and temperature are the same.

Both cure cycles in Table 5.3 were recommended by the manufacturer to achieve a full level of cure. CureA was run first, and the Force vs. Embedded Length and Force vs. Embedded Area graphs are shown in Figure 5.11a and Figure 5.11b, respectively. Initially, 21 tests were run with this cure cycle, where only seven were successful debonding tests and 14 were fiber breaks. Later more tests were run (as discussed in the following pages and in Figure 5.12), bringing the total number of tests to 26, where 11 were successful and 15 were fiber breaks. Based on the difficulty of testing and the even larger percentage of fiber breaks relative to total tests, the IFSS value for this material system was expected to be higher than that from the previous two systems discussed.

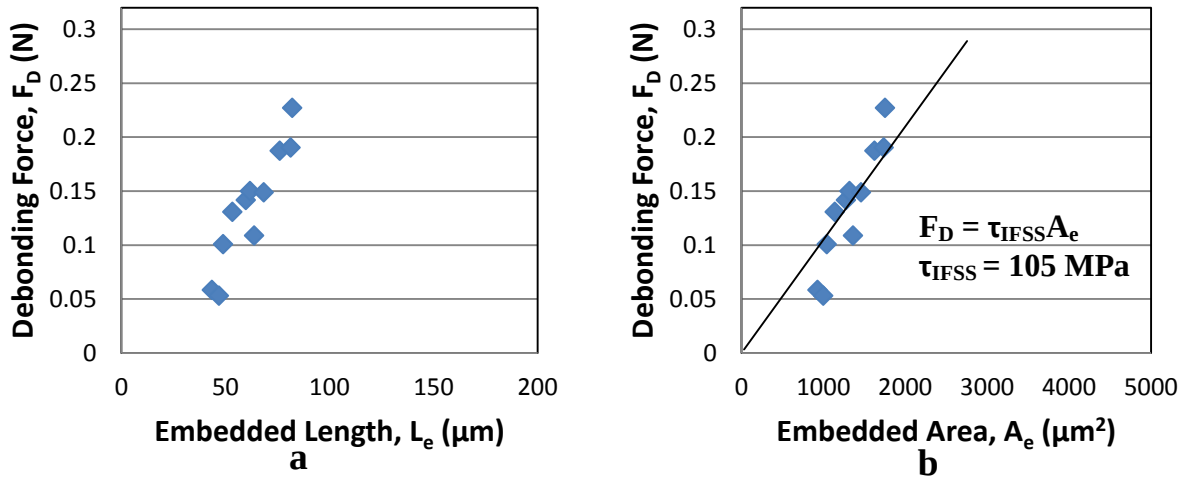

Figure 5.11 Graphs for T650/Cycom 5320-1 system cured with CureA. (a) Force vs. L_e, and (b) Force vs. A_e with regression analysis

The data for CureA shows an upward linear trend that matches up fairly well with the origin with a small amount of scatter. The IFSS value obtained from averaging the values found from Eq. (2) was 105.4 MPa, which closely matched the 105 MPa found from the regression analysis in Figure 5.11b.

The highest three data points were of particular interest in this data set. Many more specimens were tested, but over half of the specimens where the droplets had an embedded length of 60 -70 μm, and all with embedded lengths of 70 μm experience fiber breakage before debonding, so the data were not included in the IFSS calculations. The three data points on the far right of the graphs in Figure 5.11 are the exceptions to that rule. These droplets had

embedded lengths of 76, 81, and 82 μm, with IFSS of 115, 109, and129 MPa, respectively. These data points stuck out because they were successful tests among many fiber breaks, so they were investigated further.

All three of these droplets were on the same fiber, which made them even more suspect for concern. A couple explanations for why these were so different were considered. The first was that the fiber could have had a slightly larger nominal diameter, making it enough stronger that the fiber tensile strength was less than the IFSS between the fiber and the larger droplets. Another possibility was that there were actually two fibers instead of one in that specimen. In this case, the IFSS could be distributed between the two fibers, making the specimen as a whole stronger and able to withstand the IFSS better than a single fiber alone. Pictures of the specimen were taken with the stereoscopic microscope while measuring droplet embedded lengths before testing, but the image quality and magnification were not sufficient to determine for certain which hypothesis was correct. The fiber broke and disappeared while testing the last, and largest, droplet, so it could not be analyzed with the SEM to be sure. The possibility of a double fiber was then tested. Another round of tests was performed with some single fiber specimens and some double fiber specimens. This was done to be sure that the single fiber data matched with the original tests, and the double fibers could hopefully show whether the data points in question were on a single or double fiber. The double fiber specimens were purposefully made with two fibers suspended together across the metal plate and embedded in the droplets instead of one. An attempt was made to make the droplets roughly the same size as the droplets in the original round of tests, but it was difficult with the more challenging method of making droplets with the Cycom 5320-1 resin. Once the specimens were made, they were cured using CureA. Embedded lengths were then measured, and the droplets were tested. The results are shown in Figure 5.12. The blue diamond data points represent the original round of tests, while the red squares show data from the second round of tests (only successful debonding tests are shown, while data from tests where the fibers broke are not shown on the graph).

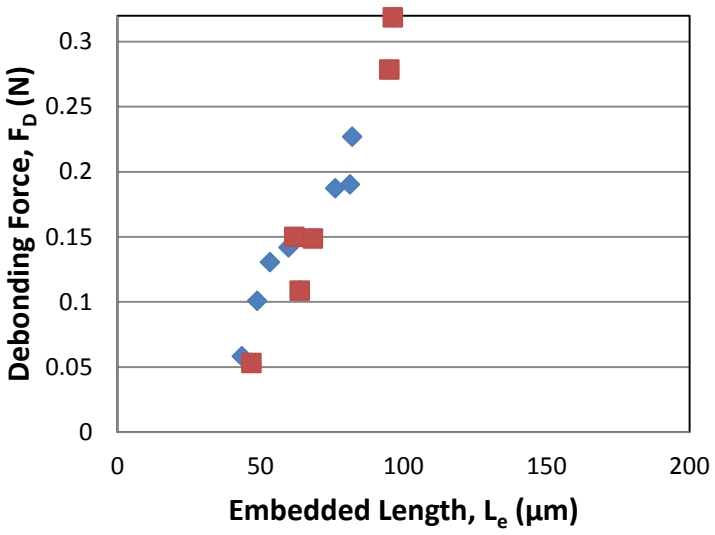

Figure 5.12 Graphs for T650/Cycom 5320-1 system cured with CureA. ◆ data from original tests. ■ data from second round of tests.

The data from the second round of tests followed a similar trend as the original test. All tests on droplets (on either single or double fibers) with embedded lengths of less than 80 µm successfully debonded. All specimens (on either single or double fibers) with droplets larger than 80 µm broke the fiber before the droplet could debond, except for two of the droplets on double fibers. The two larger droplets that debonded had embedded lengths of 95 and 96 µm. These data points from the double fibers seem to follow the same data trend as the single fiber data points, however, just as the questionable data points from the original data set did (Figure 5.12). Including the data from the single fiber specimens in the second round of tests, the IFSS value from averaging values from Eq. (2) was lower at 98.7 MPa, while the value from the regression analysis remained almost constant at 104.9 MPa.

Based on the second set of data (with both single and double fiber specimens), no significant evidence exists to exclude the three suspect data points from the original data set, so they were included in the IFSS value reported previously. It was interesting to see, however, that the known double fiber specimens with large embedded lengths that debonded successfully did not have a significantly higher IFSS as was expected. This could possibly be explained if the fibers were so close together that the embedded area did not significantly increase from single to

double fiber specimens. The two fibers together would have shared the load so they did not reach their fiber tensile strength individually before debonding occurred.

The second cure cycle used with the T650/Cycom 5320-1 material system was CureB from Table 5.3. This cure cycle had the same final cure time and temperature as CureA, but the initial cure time was significantly longer, and the initial cure temperature was also higher. According to the manufacturer, both cycles should produce fully cured specimens, so the IFSS values obtained using CureB were expected to produce values similar to those reported previously using CureA. A total of 18 tests were run with this cure cycle, where seven were successful debonding tests and 11 were fiber breaks. Graphs of data for the T650/Cycom5320-1 specimens cured with CureB are shown in Figure 5.13a and Figure 5.13b.

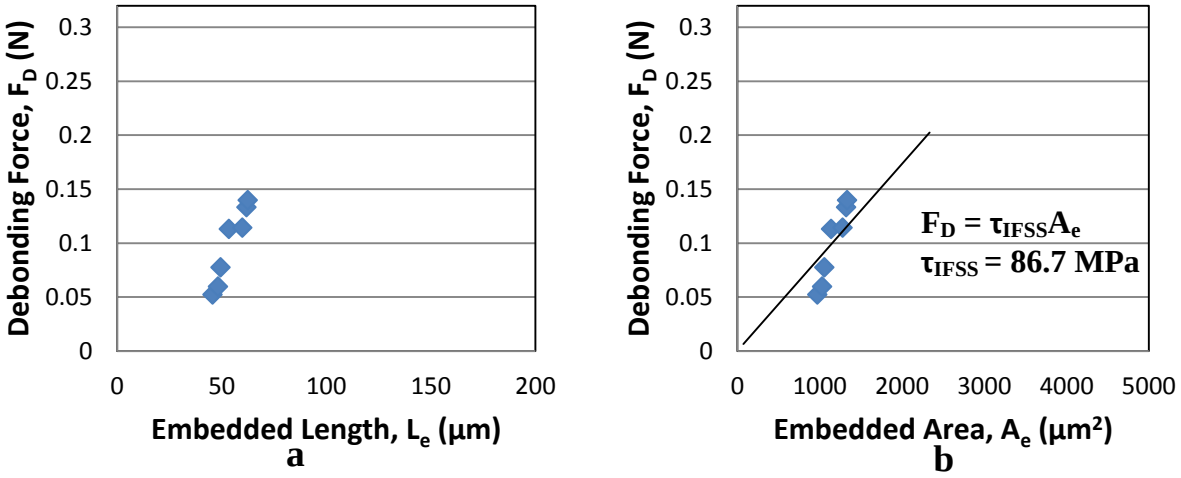

Figure 5.13 Graphs for T650/Cycom 5320-1 system cured with CureB. (a) Force vs. L_e, and (b) Force vs. A_e with regression analysis

The data points from specimens cured with CureB again displayed an upward linear trend, but this data had very little scatter. This cure cycle has fewer data points than the others, but due to the difficult nature of producing specimens, long cure cycle, high rate of fiber breakage, and very consistent results, producing and testing more samples did not seem necessary to obtain a better calculation of IFSS. For this cure cycle, the average of values found using Eq. (2) gave an IFSS value of 82.7 MPa, and regression analysis gave a value of 86.7 MPa. These values match fairly well to each other, but are about 20 MPa lower than the IFSS found using CureA.

Although both cure cycles were recommended by the manufacturer, they did not achieve the same level of cure. This shows that both steps in a cure cycle can significantly influence the final product. Even though the final step was the same for both cycles, that step in CureB could not make up for the lesser level of cure achieved by the first step. It was originally thought that the extra time the specimens spent at the lower temperature in the first step of CureB would achieve an equivalent level of cure as their counterparts in the first step of CureA with a higher temperature and shorter time. This did not turn out to be the case. Ahmadi [2] also experienced this, and explained it this way.

> "Since higher temperature forms more crosslinking points, it accelerates the curing process. On the other hand, since the diffusion velocity [26] at lower temperature is reduced, the duration of the crosslinking reaction will be prolonged. Thus, the mechanical properties at lower curing temperature do not reach the same level as for higher curing temperature even if it is cured for a longer time. [2]"

So, while the manufacturer recommended both CureA and CureB, CureA gave a noticeably higher IFSS than CureB. This shows that while both cure cycles cure the epoxy, CureA did this to a greater extent.

Chapter 6 - Conclusions and Recommendations

The purpose of this research was to determine how changes in cure cycle affected composite materials. To do this, the IFSS of three material systems were evaluated using the microbond test method. After testing and then analyzing data, it was found that cure cycle has a significant impact on IFSS. Although this statement can be made in general for carbon/epoxy composites, the amount of change in IFSS caused by different cure cycles varies for each material system. Testing the actual materials used in a specific situation is the only way to know exactly how much the final product will be affected by the change in cure cycle.

The final part of a two-step cure cycle was analyzed with the AS4/Epon828 and T650/Epon828 material systems. Increasing the final cure time from 2.0 to 2.5 hours significantly increased the IFSS, and from 2.5 to 3.0 produced a slight increase in IFSS, but increasing the cure time beyond that did not produce a higher IFSS. Therefore, increasing cure time does increase the strength of the bond between the materials to an extent, but beyond a certain point that will be different for each material system, a longer cure time does not produce a stronger material.

In analyzing the T650/Cycom 5320-1 material system, insight into how changing the initial part of the cure was gained. Although the final cure step was the same, changing the first step in the cure cycle made a significant impact on the IFSS. Starting the cure at a higher temperature for less time produced a much stronger composite than beginning with a lower temperature for a longer amount of time. Due to the chemistry of the fiber/matrix interactions, this will always be the case. How much temperature change is required to produce a noticeable change is a point of interest and would be a good follow-up to the current research.

Recommendations for further research on the AS4/Epon828 and T650/Epon828 material systems would include:

- Looking into how changing the final cure temperature affects the IFSS. Using Cure1 and Cure2 as baseline cures, alter the final cure temperature instead of time. If three variations were desired for each, change the final cure temperature by five or ten degrees to see just how much temperature change is needed to significantly change the IFSS. This could also help determine if beyond a certain temperature, a higher level of cure cannot be achieved.

- Perform similar tests as those described in this research and the previous recommendation, but on the initial cure step instead of the final cure step. This would provide more information on how much changes in initial cure affect the final composite.

Recommendations for further research on the T650/Cycom 5320-1 material system would include:

- Using CureA as a baseline cure, systematically vary initial and final cure times and temperatures as described in this research and previous recommendations.
- Using Cure1-Cure4 with this material system and compare the results with those from this research. This could provide interesting comparisons as to how the Cycom 5320-1 matrix reacts with the two different fiber types. The results could also be compared to those obtained by the manufacturer recommended cure cycles to see if using a significantly different cure cycle could also be a viable option if resources do not allow for the manufacturer-recommended cycle to be used.

References

[1] Minaie, B.*Cure management for bonded composite repair*. Wichita State University:

[2] Ahmadi, H. (2011). *Adhesion evaluation of glass fiber-PDMS interface by means of microdroplet technique.* (Unpublished MS). Kansas State University.

[3] Kelly, A. (1965). Tensile properties of fibre-reinforced metals: Copper/tungsten and copper/molybdenum. *Journal of the Mechanics and Physics of Solids, 13*, 329-350.

[4] Narkis, M., & Chen, E. (1988). Review of methods for characterization of interfacial fiber-matrix interactions. *Polymer Composites, 9*(4), 245.

[5] Bradford, D. H. (1997). *Evaluation of fiber-matrix adhesion using the single fiber fragmentation test.* (Unpublished MS). Kansas State University.

[6] Herrera Franco, P. J. (1992). Comparison of methods for the measurement of fibre/matrix adhesion in composites. *Composites, 23*(1), 2-27.

[7] Grande, D. H. (1983). *Microdebonding test for measuring Shear Strength of the Fiber/Matrix interface in composite materials.* (Unpublished M.S.). Massachusetts Institute of Technology.

[8] Broutman, L. J. (1969). Measurement of the fiber-polymer matrix interfacial strength. *Interfaces in Composites,* (ASTM STP 452), 27-41.

[9] Miller, B., Muri, P., & Rebenfeld, L. (1987). Microbond method for determination of the shear strength of a fiber/ resin interface. *Composites Science and Technology, 28*(1), 17-32.

[10] Kang, S. (2009). Fiber/epoxy interfacial shear strength measured by the microdroplet test. *Composites Science and Technology, 69*(2), 245-251.

[11] Biro, D. A., McLean, P., & Deslandes, Y. (1991). Application of the microbond technique: Characterization of carbon fiber-epoxy interfaces. *Polymer Engineering & Science, 31*(17), 1250-1256.

[12] Biro, D. (1993). Application of the microbond technique: Effects of hygrothermal exposure on carbon-fiber/epoxy interfaces. *Composites Science and Technology, 46*(3), 293-301.

[13] HexTow AS4 carbon fiber product data. (2010). Retrieved May 29, 2013, from http://www.hexcel.com/resources/datasheets/carbon-fiber-data-sheets/as4.pdf

[14] Cytec Thornel T-300 Carbon Fiber, Polyacrylonitrile (PAN) Precursor. Retrieved August 1, 2013, from http://www.matweb.com/search/datasheet.aspx?matguid=2751c19a188240ea800ba1471ab6267b.

[15] E-glass fibre. Retrieved August 20, 2013, from http://www.azom.com/article.aspx?ArticleID=764.

[16] Dupont Kevlar 49 aramid fiber. Retrieved August 20, 2013, from http://www.matweb.com/search/datasheettext.aspx?matguid=77b5205f0dcc43bb8cbe6fee7d36cbb5.

[17] Ketterer, M. E. (1984). Thermoplastic/carbon fiber hybrid yarn. *NASA Contractor Report*, http://www.dtic.mil/dtic/tr/fulltext/u2/a304536.pdf.

[18] Gaur, U. (1989). Microbond method for determination of the shear strength of a fiber/resin interface: Evaluation of experimental parameters. *Composites Science and Technology, 34*(1), 35-51.

[19] McConnell, V. (2009). The making of carbon fiber. *High Performance Composites.* 06/06/2013. Retrieved from http://www.compositesworld.com/articles/the-making-of-carbon-fiber

[20] THORNEL T-650/35 PAN-based fiber technical data sheet. (2012). Retrieved May 29, 2013, from http://www.cemselectorguide.com/pdf/THORNEL_T650-35_052112.pdf

[21] Hexion EPON resin 828 technical data bulletin. (2005). Retrieved June 27, 2013, from http://www.silmid.com/getattachment/1d433cac-6b49-4f35-ac0c-b52f6501c22d/Epon-828.aspx

[22] CYCOM 5320-1 epoxy resin system technical data sheet. (2012). Retrieved April 17, 2013, from http://www.cemselectorguide.com/pdf/CYCOM_5320-1_031912.pdf

[23] Nishikawa, M. (2008). Micromechanical modeling of the microbond test to quantify the interfacial properties of fiber-reinforced composites. *International Journal of Solids and Structures, 45*(14), 4098-4113.

[24] Gu, X. (1997). Deformation micromechanics in model carbon fiber reinforced composites part II: The microbond test. *Textile Research Journal, 67*(2), 93-100.

[25] Maurin, R. (2008). *Influence of epoxy curing cycle on microdamage. comparison between glass/epoxy and carbon/epoxy using multiscale tests.*

[26] Deushle, J.K., Et al. (2010). Nanoindentation studies on crosslinking and curing effects of PDMS. *International Journal of Materials Research*. 101: 1014-1023.

Appendix A - Detailed Procedure for Preparing Specimens

The processes for making the specimens were very tedious and sensitive. While the processes were described in Chapter 3, more detailed descriptions are given here.

AS4/Epon828 and T650/Epon828 Specimens

Preparing Fibers

- Cut a piece of white paper to fit in the bottom of a petri dish or other small storage container.
- Using scissors, cut a small bundle of fibers about one and a half inches in length from the fiber tow.
- Using tweezers, transfer the small fiber bundle to the paper in the storage container.
- With a pair of tweezers in each hand, carefully separate the fibers into smaller bundles in the container. This will make it easier to get single fibers later.
- Obtain a small metal piece with a hole in the middle. A small rectangular piece with a 2 cm hole was used in this research. Place a piece of double-sided tape on either side of the hole.
- Again using the tweezers, carefully separate a single fiber from a small group of fibers. This can be difficult as the fibers break easily and like to stick together. Using a small head lamp with magnifying glass can make this process easier. Use the magnifying glass to be sure there is only one fiber.
- Carefully grab both ends of the fiber with the tweezers and place one end on each piece of tape on the metal plate. Do not squeeze the fiber too hard, or it will break! Align the fiber with the edges of the plate as much as possible. This will make measuring embedded lengths easier later on. The best way to do this is to line the fiber up above the plate, then put one end on the tape. Gently press on that end with the side of the tweezers to secure it to the tape without breaking it. Slowly lower the other end to the tape with the tweezers, pulling it just a little to ensure it is tight. Sagging fibers make depositing droplets and measuring them later more difficult, so it is best to make sure they are snug across the tape. Again, gently press on the fiber with the side of the tweezers to secure the second end to the tape.

- Repeat this process with more fibers. In this research, 6-10 fibers were generally put on each plate. A picture of the plate with three fibers is shown in Figure A.1.
- Once the fibers are suspended and ready for droplets, prepare the epoxy.

Preparing Epon828

- Place a clean plastic cup on a scale. In this research, an Explorer Pro analytical balance from OHAUS was used. Zero the scale with the cup on it.
- Transfer 3-5g of bisphenol A diglycidyl ether to the cup.
- Using a small pipette or other small-scale measuring device, transfer about 12% of the diethylenetriamine hardener into the cup. In this research, a function on the scale measured the weight ratios as material was added.
- Stir the two liquids together with a clean glass rod until many small bubbles are present in the mixture. This ensures the materials have mixed properly.
- Let the epoxy rest for about 5-10 minutes, or until the bubbles are no longer present. While the epoxy is resting, prepare your wire. In this research, a small coated wire was used to transfer epoxy to the fibers, but the end of the wire was sanded prior to use to remove the coating and create as fine a point as possible. This was usually done while the epoxy was resting. A picture of the sanded wire lying on a plate with fibers suspended is shown in Figure A.1.

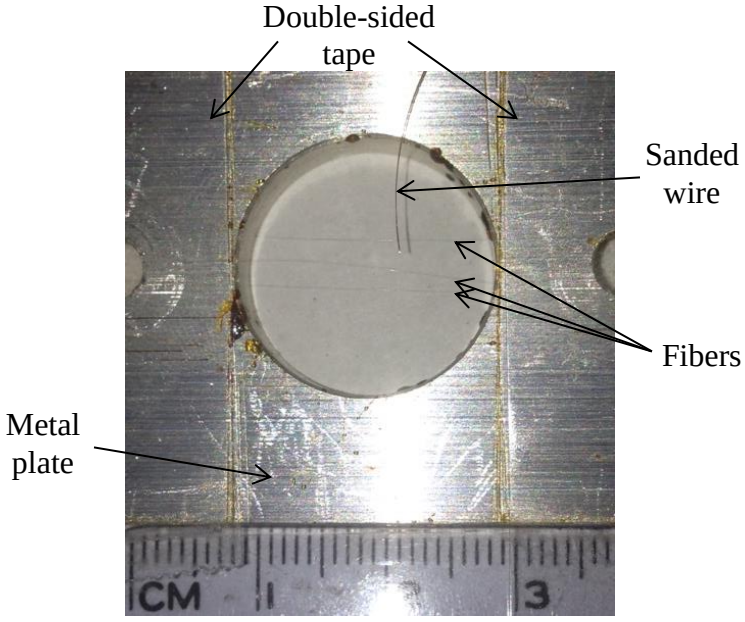

Figure A.1 Close-up of plate with fibers suspended and sanded wire lying on top.

Making Specimens

- Once the bubbles are no longer present in the epoxy, dip the sanded end of the wire into the epoxy. A drop of epoxy should be attached to the wire when it is removed from the epoxy. If not, dip the wire again. If the droplet is too large and wants to slide off of the wire, touch the droplet to the side of the cup to remove some of it.
- With the droplet on the wire, carefully slide the droplet along a fiber suspended across the plate. Do this several times until many small droplets remain along the length of the fiber. (Most of the length of the fiber should have many droplets of varying sizes along it.)
- Remove the majority of the epoxy remaining on the wire by touching it again to the inside of the cup containing the epoxy.
- Look at the droplets on the fiber and determine which ones need removed, and which will be kept. In this research, droplets with embedded lengths of 30-130 μm were used. In general, about four droplets per fiber were kept. The droplets needed to be separated by several millimeters to accommodate the knife edges during testing. An example of a fiber with many droplets and the selection process used to determine which droplets to keep is shown in Figure A.2. Determining which droplets to keep takes practice. The droplets in the figure have the embedded lengths measured to show examples of droplet sizes, but of course they do not have measurements after being formed. It takes practice, some trial and error, and a few iterations to know just by looking at them about how large they are.

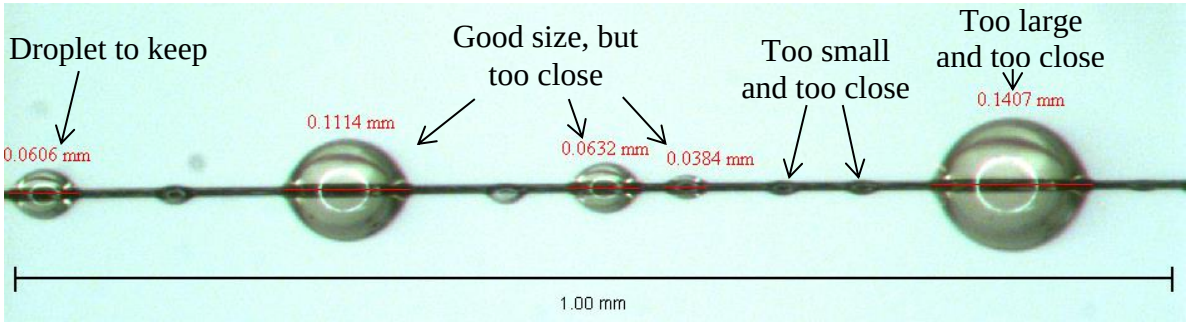

Figure A.2 Part of a typical fiber after the large drop of epoxy was swept across it and formed droplets, but before unwanted droplets were removed.

- Using the same wire, remove the unwanted droplets. This is easiest if there is still a little epoxy on the wire. To remove the droplets, touch them with the wire. They should come off of the fiber and stick to the wire. Remove all of the unwanted droplets. There is likely some residual resin around the droplet to keep. Measuring and aligning knife edges is easier when this is removed, so with a small amount of epoxy still on the wire, carefully touch it to the wire and slide it slowly toward the droplet. Get as close as possible without touching the droplet and then pull the wire away from the fiber. Again this process takes practice to move it slow enough not to deposit more droplets as well as to not touch and remove the droplet that was meant to stay.
- Repeat this process for all fibers suspended on the plate. The specimens are now ready to be cured.

T650/Cycom 5320-1 Specimens

Preparing Fibers

The same fiber preparation technique was used for these specimens as was described above for the other two material systems. After all fibers were suspended, a second layer of tape was applied over top to keep the fibers in place when depositing droplets.

Preparing Cycom 5320-1

The Cycom 5320-1 matrix was supplied as a B-stage epoxy in film form. Each film was on a separate sheet of special paper. The matrix had to be kept in a freezer until used as it would begin to cure at room temperature. The process to apply droplets to fibers is described in the following section.

Making Specimens

- Using a piece of aluminum foil, make a small "boat" that will accommodate a microscope slide or other glass surface.
- Retrieve a sheet of matrix from the freezer. Using small scraper tools, remove a small amount of matrix from the paper (several small globs about the size of pin heads work well). The longer the epoxy is out of the freezer, the stickier it gets, so it is best to do this

process quickly to avoid it sticking to the scrapers. Place epoxy globs on the microscope slide and return the rest of the epoxy to the freezer.

- Turn on a hot plate and heat to the temperature of the initial cure step of the cure cycle. Place the foil boat on the hot plate and put the microscope slide with epoxy in the boat. Place the metal plate with suspended fibers on the hot plate as well. This allows the fibers to be heated as well which helps with droplet formation.
- While the epoxy is heating, prepare the wire (same wire and preparation as described previously).
- Wait for the epoxy to heat. It is warm enough when the wire can be dipped into the globs and a string of matrix is attached when removed. This usually takes around 10 minutes. When it is warm enough, dip the end of the wire in a pool of epoxy and transfer the attached string to a fiber. Move the wire to the fiber as quickly as possible as the epoxy cools quickly during the transfer. Once the epoxy is on the fiber, carefully pull the wire away. If the wire is removed too quickly, the sticky matrix will sometimes try to stay with both it and the fiber and the fiber will break.
- See how much epoxy is on the fiber and transfer more if necessary. As with the Epon828 specimens, the goal is to end up with about four droplets per fiber in the 30-130 μm range.
- The strings of epoxy should separate into droplets on the fiber if they are close enough to the heat source. Once this happens, remove unwanted droplets. This is done using the same technique as described for the Epon828 specimens, but has to be done more gently. The Cycom 5320-1 epoxy is not as viscous and sticks more to the fibers. To remove unwanted epoxy from the fiber, carefully touch the wire to it for a second. Pull the fiber away from the wire very slowly, making sure the epoxy is coming away with it. Sometimes it helps to heat the wire on the hot plate itself just before touching the wire to the unwanted epoxy. This heats it a little more, making it easier to work with and more apt to come off the fiber.
- Repeat the process for all fibers. Once the droplets are prepared, they are ready to be put in the oven for the remainder of the cure cycle.